University of Szeged

Albert Szent-Györgyi Medical School

Doctoral School of Experimental and Preventive Medicine

The role of SPCA2 in store-independent STIM1-ORAI1 activation and the regulation of basal CFTR activity in epithelial secretion

Ph.D. Thesis

Aletta Kata Kiss

Supervisor:

József Maléth M.D., Ph.D.

Szeged

2025

1. TABLE OF CONTENTS

2. LIST OF PUBLICATION RELATED TO THE THESIS

I. Store-independent activation of STIM1-ORAI1 by SPCA2 determines the basal CFTR activity in secretory epithelial cells

Aletta Kata Kiss*, Árpád Varga*, Marietta Görög, Tamara Madácsy, Woo Young Chung, Petra Pallagi, Viktória Szabó, Petra Susánszki, Enikő Kúthy-Sutus, Dániel Varga, Péter Bíró, Ingrid Hegnes Sendstad, Tim Crul, Boldizsár Jójárt, Bálint Tél, Zsófia Horváth, Szintia Barnai, Anita Balázs, György Lázár, Miklós Erdélyi, Shmuel Muallem, József Maléth

Current Biology 35: 20 pp. 4970-4987.e7., 25 p. **(2025)**; MTMT ID: 36356148

IF: 7.5 (D1)

II. Human Pancreas-Derived Organoids with Controlled Polarity: Detailed Protocols and Experimental Timeline

Aletta Kiss, Attila Farkas, Ferhan Ayaydin, György Lázár, Árpád Varga, József Maléth

Current Protocols 4: 11 Paper: e70045, 25 p. **(2024)**; MTMT ID: 35609714

IF: 2.2 (D1)

3. LIST OF PUBLICATION NOT RELATED TO THE THESIS

I. Impaired regulation of PMCA activity by defective CFTR expression promotes epithelial cell damage in alcoholic pancreatitis and hepatitis

Madácsy Tamara, Varga Árpád, Papp Noémi, Tél Bálint, Pallagi Petra, Szabó Viktória, **Kiss Aletta**, Fanczal Júlia, Rakonczay Zoltan, Tiszlavicz László, Rázga Zsolt, Hohwieler Meike, Kleger Alexander, Gray Mike, Hegyi Péter, Maléth József

CELLULAR AND MOLECULAR LIFE SCIENCES **(D1)**; DOI:

IF: 9.207

II. Thiopurines impair the apical plasma membrane expression of CFTR in pancreatic ductal cells via RAC1 inhibition

Tél Bálint, Papp Noémi, Varga Árpád, Szabó Viktória, Görög Marietta, Susánszki Petra, Crul Tim, **Kiss Aletta**, Sendstad Ingrid H, Bagyánszki Mária, Bódi Nikolett, Hegyi Péter, Maléth József, Pallagi Petra

CELLULAR AND MOLECULAR LIFE SCIENCES **(D1)**; DOI:

IF: 9.234

III. Orai1 calcium channel inhibition prevents progression of chronic pancreatitis

Szabó Viktória, Csákány-Papp Noémi, Görög Marietta, Madacsy Tamara, Varga Árpád, **Kiss Aletta**, Tel Balint, Jójárt Boldizsár, Crul Tim, Dudás Krisztina, Bagyánszki Mária, Bódi Nikolett, Ayaydin Ferhan, Jee Shyam, Tiszlavicz Laszlo, Stauderman Kenneth A., Hebbar Sudarshan, Pallagi Petra, Maléth József
JCI Insight **(DI)**; DOI:
IF: 9,484

IV. Human pancreatic ductal organoids with controlled polarity provide a novel ex vivo tool to study epithelial cell physiology
Árpád Varga, Tamara Madácsy, Marietta Görög, **Aletta Kiss**, Petra Susánszki, Viktória Szabó, Boldizsar Jojart, Krisztina Dudás, Gyula Jr. Farkas, Edit Szederkényi, György Lázár, Attila Farkas, Ferhan Ayaydin, Petra Pallagi, József Maléth
CELLULAR AND MOLECULAR LIFE SCIENCES **(D1)**; DOI:
IF: 9.234

Number of full publications: 6 (2 first author publication)

Cummulative IF: 46.859

4. LIST OF ABBREVIATIONS

AC/ADCY – Adenylyl cyclase

AKAP – A-kinase anchoring protein

ATP – Adenosine triphosphate

ATCC – American Type Culture Collection

BAPTA – 1,2-bis(o-aminophenoxy)ethane-N,N,N′,N′-tetraacetic acid (a calcium chelator)

BSA – Bovine serum albumin

BCECF – 2',7'-bis-(2-carboxyethyl)-5-(and-6)-carboxyfluorescein (fluorescent dye)

Ca^{2+} – Calcium

CaMKII – Calcium/calmodulin-dependent protein kinase II

cAMP – Cyclic adenosine monophosphate

cDNA – Complementary DNA

CF – Cystic fibrosis

CFTR – Cystic fibrosis transmembrane conductance regulator

Cl^- – Chloride

CPA – Cyclopiazonic acid (SERCA inhibitor)

D1ER – D1ER genetically encoded calcium indicator protein

DMEM – Dulbecco's Modified Eagle Medium

DPBS – Dulbecco's phosphate-buffered saline

dSTORM – Direct Stochastic Optical Reconstruction Microscopy

ECL – Enhanced chemiluminescence

EGF – Epidermal growth factor

EGTA – Ethylene glycol-bis(β-aminoethyl ether)-N,N,N′,N′-tetraacetic acid (calcium chelator)

ER – Endoplasmic reticulum

FACS – Fluorescence-activated cell sorting

FBS – Fetal bovine serum

FGF – Fibroblast growth factor

FLIM – Fluorescence lifetime imaging microscopy

FRET – Förster resonance energy transfer

GAPDH – Glyceraldehyde 3-phosphate dehydrogenase

GFP – Green fluorescent protein

GPCR – G protein-coupled receptor

HA – Hemagglutinin tag (epitope tag)

HBSS – Hank's Balanced Salt Solution

HCO_3^- – Bicarbonate

HEK293 – Human embryonic kidney 293 cells

HEPES – 4-(2-hydroxyethyl)-1-piperazineethanesulfonic acid (buffer)

IF – Immunofluorescence

KRT19 – Keratin 19

KO – Knockout

L-WRN – Cell line producing WNT, R-spondin, and Noggin factors

MSD – Membrane-spanning domain

mCherry – mCherry fluorescent protein

mRNA – Messenger RNA

NaCl – Sodium chloride

NBD – Nucleotide-binding domain

NHERF1 – Na^+/H^+ exchanger regulatory factor 1

OC/OCs – Organoid culture/organoids

Opti-MEM – Optimized Minimal Essential Medium

ORAI1 – Calcium release-activated calcium channel protein 1

PBS – Phosphate-buffered saline

PDE – Phosphodiesterase

PFA – Paraformaldehyde

PKC – Protein kinase C

PKA – Protein kinase A

qRT-PCR – Quantitative reverse transcription polymerase chain reaction

PVDF – Polyvinylidene difluoride membrane

RNA-Seq – RNA sequencing

ROI – Region of interest

R domain – Regulatory domain (CFTR)

RIPA – Radioimmunoprecipitation assay (buffer)

SICE – Store-independent calcium entry

SLC26 – Solute carrier family 26

SOCE – Store-operated calcium entry

SPCA1/2 – Secretory pathway Ca^{2+}-ATPase isoform 1/2

STIM1 – Stromal interaction molecule 1

TIRF – Total internal reflection fluorescence

TPM – Transcripts per million

YFP – Yellow fluorescent protein

5. INTRODUCTION

5.1. Epithelial ion and fluid secretion

Secretory epithelial cells represent a fundamental cellular component governing fluid and ion homeostasis across diverse organ systems throughout the mammalian body (1,2). These highly specialized cells, which line the ductal networks and luminal surfaces of exocrine organs including the respiratory tract, pancreatic ductal system, hepatobiliary tree, salivary glands, and sweat glands, orchestrate the precise transport of electrolytes – particularly chloride (Cl^-) and bicarbonate (HCO_3^-) (2) – alongside water movement into luminal compartments (3,4) **(Figure 1.)**.

This vectorial transport process serves multiple critical physiological functions: maintaining optimal hydration of mucosal surfaces, facilitating mucociliary clearance mechanisms in pulmonary tissues, supporting digestive enzyme function in gastrointestinal contexts, enabling thermoregulatory sweat production in cutaneous tissues, and preserving the ionic composition of various secretory fluids (5,6).

Defective epithelial secretion underlies a broad spectrum of human diseases, ranging from the life-threatening manifestations of cystic fibrosis (CF) to chronic pancreatitis, autoimmune exocrinopathies such as Sjögren's syndrome, and various secretory diarrheal conditions. The multi-organ impact of epithelial transport defects illustrates how proper baseline activity of secretory epithelia represents an essential prerequisite for human health and survival (2,7,8).

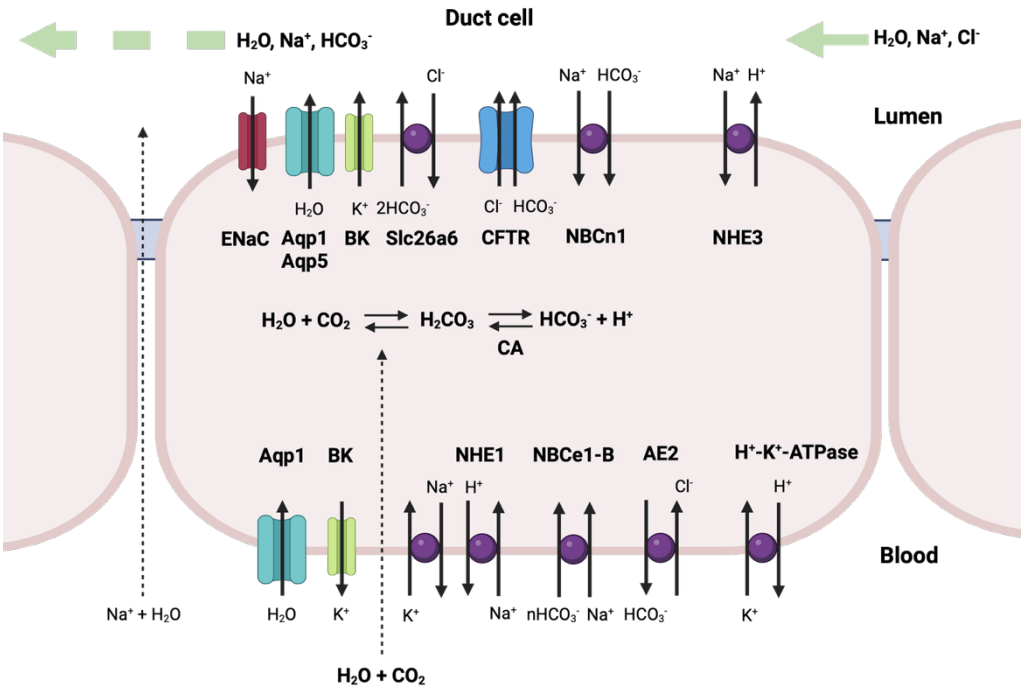

Figure 1. Schematic figure of the ductal fluid and HCO_3^- secretion in pancreatic duct cell. Schematic representation based on Lee et al. (2012) (9), generated using BioRender.

5.2. The central role of CFTR in epithelial ion transport

Among the molecular components involved in the transepithelial ion and fluid secretion, the cystic fibrosis transmembrane conductance regulator (CFTR) Cl^- channel plays a central role in the epithelial physiology (7,10). CFTR functions as a selective Cl^- and HCO_3^- channel localized predominantly on the apical membrane of epithelial cells, where it serves as the rate-limiting step for fluid secretion across multiple organ systems (2,10,11). The activation of CFTR permits the controlled efflux of Cl^- and HCO_3^- ions into the luminal space, which in turn drives the paracellular movement of sodium through electrochemical coupling mechanisms and promotes osmotic water transport across the epithelial barrier, ultimately resulting in coordinated fluid secretion (4). The physiological significance of CFTR extends far beyond simple ion conduction, as this channel protein plays a pivotal regulatory role in maintaining both the hydration status and pH homeostasis of epithelial secretions (7,12). The importance of CFTR function becomes starkly apparent in CF, where loss-of-function mutations in the CFTR gene result in profound alterations in secretory physiology across multiple organ systems (13). In CF patients, the absence of functional CFTR leads to the production of abnormally dehydrated and acidic mucus in respiratory and gastrointestinal tracts, enzyme precipitation and ductal obstruction in pancreatic tissues, and the characteristic production of excessively concentrated, sodium chloride (NaCl)-rich sweat (10,14). These multi-organ manifestations illustrate the universal importance of CFTR-mediated transport in maintaining epithelial function and demonstrate how aberrant epithelial fluid secretion can have far-reaching consequences for human health.

5.3. Molecular regulation of CFTR

CFTR is organized into four functional units: two membrane-spanning domains (MSD1 and MSD2) containing six transmembrane helices each, which form the channel pore; two nucleotide-binding domains (NBD1 and NBD2) located in the cytoplasm; and a regulatory (R) domain with intrinsic disorder that links NBD1 to MSD2 and governs channel gating (10,15).

The channel's gating mechanism is tightly controlled by the R domain, which in its unphosphorylated state occupies an inhibitory position that prevents dimerization of the NBDs and subsequent channel opening (16,17). The canonical activation pathway for CFTR involves the cyclic adenosine monophosphate (cAMP)/protein kinase A (PKA) signalling cascade. Following stimulation of G protein-coupled receptors (GPCRs), particularly β_2-adrenergic receptors localized at the apical membrane of polarized epithelial cells, adenylyl cyclases (ACs) catalyse the conversion of ATP to cAMP (18,19). The resulting cAMP elevation activates PKA, which phosphorylates multiple serine residues within the CFTR R domain, including S422, S660, S795, and S813 (20–22). This phosphorylation relieves the autoinhibitory constraint imposed by the R domain, facilitating NBD dimerization and channel opening with up to a 100-fold increase in open probability (17,21,23,24).

Recent structural and functional studies have revealed that CFTR activation by PKA occurs through dual mechanisms. Beyond the well-established phosphorylation-dependent catalytic activation, PKA can also activate CFTR through simple binding in a phosphorylation-independent manner. This noncatalytic activation mechanism involves direct PKA-CFTR interaction that promotes release of the unphosphorylated R domain from its inhibitory position, resulting in full channel activation that is completely reversible upon PKA dissociation (21,25). These findings suggest multiple levels of CFTR regulation in cells, with reversible control mediated by PKA binding and irreversible sustained activity maintained through phosphorylation (26).

The spatial organization of CFTR signalling involves the formation of macromolecular complexes organized by scaffolding proteins, particularly A-kinase anchoring proteins (AKAPs) and Na^+/H^+ exchanger regulatory factor 1 (NHERF1). The AKAP ezrin establishes a physical connection between PKA and CFTR, and this interaction is essential for the full PKA-dependent activation of the channel. Disrupting ezrin-based anchoring results in an 83% reduction in membrane conductance in airway epithelial cells (22). In addition, NHERF1 increases the stability of CFTR at the apical membrane by linking it to ezrin and the underlying actin cytoskeleton. This connection slows channel internalization through endocytosis and promotes its prolonged retention at the cell surface (27). CFTR inactivation occurs through three complementary mechanisms: GPCR desensitization, phosphatase-mediated dephosphorylation, and cAMP degradation by phosphodiesterases (PDEs). The PDE4 isoform plays a predominant role by tightly regulating cAMP diffusion around CFTR via direct protein–protein interactions in airway epithelial cells. This local control of cAMP levels ensures precise

temporal regulation of CFTR activity and prevents unintended activation of other cAMP-dependent pathways. (28,29).

5.4. The role of Ca^{2+} signalling in CFTR regulation

While the cAMP/PKA pathway remains the primary mechanism for CFTR activation, accumulating evidence indicates that calcium (Ca^{2+}) signalling provides critical complementary regulation of channel function (20,30,31). The interplay between cAMP and Ca^{2+} pathways is particularly evident in secretory epithelia, where both second messengers contribute to the coordination of fluid and electrolyte secretion. Ca^{2+} can modulate CFTR activity through multiple mechanisms **(Figure 2.)**. The Ca^{2+}-binding protein calmodulin directly interacts with CFTR and enhances its open probability in a Ca^{2+}-dependent manner. This calmodulin-mediated regulation shares similarities with PKA-dependent activation, as both involve relief of R domain-mediated autoinhibition (32,33). Additionally, Ca^{2+}-activated kinases including Ca^{2+}/calmodulin-dependent protein kinase II (CaMKII) and Src-family tyrosine kinases can phosphorylate CFTR at distinct sites, providing parallel regulatory pathways. A critical node of cAMP-Ca^{2+} crosstalk occurs at the level of ACs, the enzymes responsible for cAMP synthesis. The mammalian AC family comprises nine membrane-bound isoforms with distinct regulatory properties. Notably, AC1, AC3, and AC8 are stimulated by Ca^{2+}/calmodulin, while AC5 and AC6 are inhibited by Ca^{2+} through PKC-dependent and -independent mechanisms (34). This differential Ca^{2+} sensitivity allows fine-tuning of local cAMP production in response to intracellular Ca^{2+} fluctuations. The spatial organization of AC isoforms contributes to the generation of distinct cAMP microdomains. Studies have shown that Ca^{2+}-regulated ACs localize to lipid rafts in the plasma membrane, positioning them to respond to localized Ca^{2+} signals (30). In bronchial epithelial cells, colocalization of AC1 with CFTR at the apical membrane supports the existence of functional coupling between Ca^{2+}-activated cAMP production and CFTR activation (35). However, the specific contributions of individual AC isoforms to CFTR regulation in different epithelial cell types remain incompletely understood.

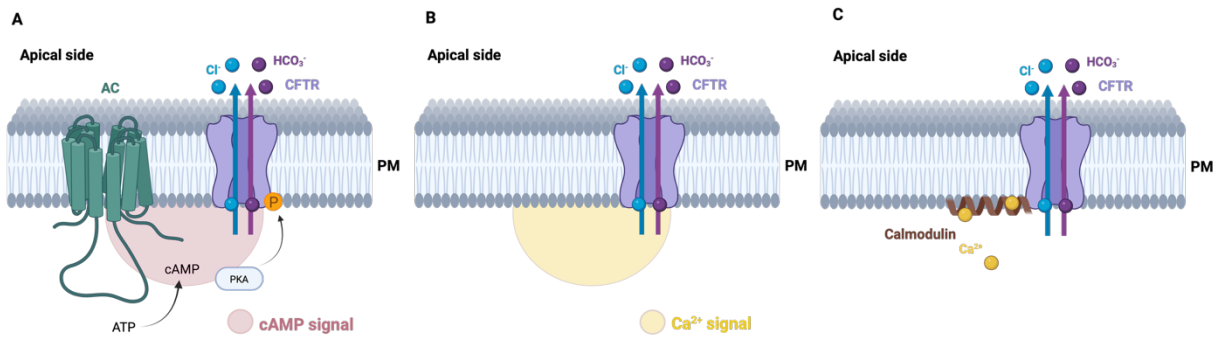

Figure 2. Known mechanisms of CFTR activation. **(A)** CFTR activation via cAMP produced by ACs and subsequent PKA-mediated phosphorylation. **(B)** CFTR activation regulated by intracellular Ca^{2+} levels or **(C)** mediated by the Ca^{2+}-binding protein calmodulin. Illustration based on Bozoky et al (2017) (32) and created with BioRender.

Recent work has highlighted the importance of Ca^{2+} signalling in epithelial HCO_3^- secretion, a process critically dependent on CFTR function (33). In pancreatic ductal epithelial cells, CFTR mediates both Cl^- and HCO_3^- transport, with HCO_3^- secretion playing an essential role in maintaining alkaline pancreatic juice. The regulation of this process involves complex interactions between CFTR, Cl^-/HCO_3^- exchangers (SLC26 family), and the WNK1/SPAK kinase pathway, all of which are modulated by Ca^{2+}-dependent mechanisms (30,36).

5.5. Store-operated and store-independent Ca^{2+} entry in epithelial cells

The primary mechanism for Ca^{2+} entry in non-excitable cells, including epithelial cells, is store-operated calcium entry (SOCE), mediated by the ORAI family of Ca^{2+} channels and the stromal interaction molecule (STIM) proteins (37). Upon depletion of endoplasmic reticulum (ER) Ca^{2+} stores, STIM1 senses the decline in luminal Ca^{2+} concentration, oligomerizes, and translocates to ER-plasma membrane junctions where it directly binds and activates ORAI1 channels (37–39). The resulting Ca^{2+} influx serves dual functions of refilling ER stores and triggering Ca^{2+}-dependent cellular responses (40). In airway epithelial cells, SOCE plays critical roles in inflammatory cytokine production, regulation of ciliary beat frequency, and mucin secretion (41). Both ORAI1 and STIM1 are highly expressed in primary bronchial epithelial cells and cell lines, and their knockdown or pharmacological inhibition strongly suppresses Ca^{2+} entry. The resulting Ca^{2+} signals can vary from oscillations to sustained elevations depending on the stimulus and cell type, reflecting the versatility of SOCE in encoding different physiological responses. Beyond the canonical SOCE pathway, emerging evidence points to store-independent calcium entry (SICE) mechanisms involving ORAI1 (36,40,42–44). A key player in SICE is the secretory pathway Ca^{2+}-ATPase isoform 2 (SPCA2), which, unlike the ubiquitously expressed SPCA1, can traffic to the plasma membrane and directly interact with ORAI1 (45). This SPCA2-ORAI1 interaction activates Ca^{2+} influx independently of ER store depletion and STIM proteins and is uncoupled from the Ca^{2+}-ATPase activity of SPCA2 (46). The short C-terminal domain (26 amino acids) of SPCA2 is sufficient to mediate this interaction and gate ORAI1 channels, possibly through electrostatic interactions (47). SPCA2-mediated SICE has been demonstrated in several physiological contexts. In lactating mammary glands,

co-induction and co-immunoprecipitation of SPCA2 and ORAI1 support elevated basolateral Ca^{2+} influx necessary for milk secretion (48,49). Knockdown of either SPCA2 or ORAI1 severely depletes Ca^{2+} influx and interferes with mammosphere differentiation. In breast cancer cells, ectopic expression of SPCA2 or its C-terminal activating domain elevates cytosolic Ca^{2+} levels sufficiently to drive transformation, an effect mediated through constitutive SPCA2-ORAI1 interaction and activation of the RAS-ERK signalling pathway (44,45,49–51).

Despite the recognized importance of ORAI1-mediated Ca^{2+} entry in various cell types and the established role of Ca^{2+} in modulating CFTR activity, the potential contribution of ORAI1 to CFTR regulation in epithelial cells has not been systematically investigated. Given the colocalization of CFTR and Ca^{2+}-sensitive ACs at the apical membrane, and the emerging recognition of SICE mechanisms, it is plausible that ORAI1 channels contribute to the local Ca^{2+} microdomains that regulate CFTR function.

5.6. Organoid models as tools for studying epithelial physiology

The study of epithelial ion transport mechanisms has been significantly advanced by the development of three-dimensional organoid culture systems. Organoids are self-organizing structures derived from embryonic, induced pluripotent, or adult tissue-specific stem cells that recapitulate key aspects of their parent organ's architecture and function (52,53). Adult stem cell-derived organoids, particularly those established from $Lgr5^+$ cells, have proven especially valuable for investigating epithelial physiology and disease mechanisms (54–56). Organoid cultures offer several advantages over traditional two-dimensional cell culture systems. They maintain epithelial polarity, with proper segregation of apical and basolateral membrane domains, and contain multiple differentiated cell types that interact in physiologically relevant ways (52,57–59). For CFTR research, this is particularly important as the channel's function depends critically on its apical localization and interaction with other membrane proteins. Organoids can be established from pancreas, lung, liver, and intestine, the major organs affected in CF, providing tissue-specific models for investigating CFTR regulation (60–63). Maintenance of organoid cultures requires an extracellular matrix scaffold (typically Matrigel or similar products) and a defined medium containing key niche factors including WNT ligands, R-spondin, and Noggin (55,64,65). These factors maintain the stem cell niche by activating the WNT/β-catenin signalling pathway and inhibiting BMP-mediated differentiation. The resulting cultures can be maintained long-term through serial passaging while retaining their epithelial

identity and functional characteristics. For pancreatic ductal organoids specifically, the cultures express characteristic ductal markers (CFTR, KRT19, OCLN, SOX9) and exhibit morphological features like native ducts, including apical mitochondrial enrichment and brush border formation (59,66).

The applicability of organoid models to investigating CFTR regulation is supported by their preservation of native protein-protein interactions and signalling microdomains. Unlike immortalized cell lines or overexpression systems, organoids maintain endogenous expression levels and stoichiometry of regulatory proteins, providing a more accurate representation of *in vivo* regulation. This makes them particularly suitable for investigating questions about the molecular organization and functional coupling of signalling pathways in polarized epithelial cells.

6. AIMS

1. We aimed to characterize the store-independent activation of STIM1–ORAI1 by SPCA2 and to evaluate the physiological relevance of this signalling nanodomain in polarized secretory epithelial cells from multiple tissues, including the pancreas, airways, and liver.

2. We also aimed to determine how SPCA2-mediated Ca^{2+} influx regulates basal CFTR activity via Ca^{2+}-sensitive ACs and local cAMP signalling.

3. We aimed to standardize the experimental use of human organoid cultures as a model for epithelial fluid and ion secretion in primary, polarized epithelia.

7. MATERIALS AND METHODS

7.1. Cell lines and animals

HeLa and HEK293 cells were grown in DMEM containing 10% fetal bovine serum (FBS), 1% Kanamycin Sulfate, 1% Antibiotic-Antimycotic solution, and 1% GlutaMax™ supplement. Conditioned medium for organoid cultures has been provided by L-WRN cell line grown in selection medium containing 10% FBS and 0.5-0.5 mg/ml G418 and Hygromycin B in ATCC-formulated DMEM. Conditioned medium has been collected a total of three times every three days and pooled before further applications.

8- to 12-week-old and 20-25-gram weighted FVB/N mice were used during all the experiments. Animals were kept at a constant room temperature (22-24°C) with a 12-hour light-dark cycle. Mice were allowed free access to rodent chow. The gender ratio was 1:1 for all investigated groups.

7.2. Isolation of pancreatic ductal fragments and acinar cells

Pancreatic ductal fragments were isolated as described earlier (67,68). Briefly, terminal anesthesia with pentobarbital was followed by surgical removal of the pancreas. Pancreatic tissue was partially digested in a vertical shaker with enzymatic solution for 30 mins at 37ºC. Small intra-/interlobular ducts were identified and isolated by microdissection under a stereomicroscope. The tissue was minced into 1-3 mm^3 pieces for pancreatic acinar cell isolation and placed in ice-cold HBSS. Lipids and fats were removed by centrifugation at 450 RCF (Rotor radius: 180 mm) for 2 min. Tissue pieces were digested at 37°C for 20 min as described previously (69,70). Digested tissue was washed by HBSS at 4°C. The supernatant was centrifuged for 2 min at 450 RCF (Rotor radius: 180 mm), and the pellet was resuspended in DMEM/F12 with 2.5% FBS, 2 mM glutamine, and 0.25 mg/ml soybean trypsin inhibitor.

7.3. Mouse and human organoid cultures

Human pancreatic tissue samples were collected from cadaver donors. For mouse organoid cultures (OCs), after terminal anesthesia by pentobarbital, pancreatic, liver, and lung tissue were removed from the animals surgically and placed in splitting media. Mouse and human tissues were minced into small fragments and incubated at 37°C in a digestion solution in a vertical shaker for approximately 1h, depending on tissue density. The efficiency of the digestion

process was verified by stereomicroscopy every 10 minutes. Cells were collected (200 RCF, 10 min, 4ºC, Rotor radius: 180 mm) and washed twice by Wash Media. Resuspended cells in Wash media were mixed with Matrigel in a ratio of 1:5. Matrigel domes (10 µl) were placed in one well of a 24-well cell culture plate. After 10 minutes of solidification at 37ºC, 500 µl Feeding Media were applied in each well. Feeding media was changed every second day. For OC passaging, domes were pooled and collected (200 RCF, 10 min, 4ºC, Rotor radius: 180 mm). Matrigel removal and cell separation were performed simultaneously by using TrypLE™ Express Enzyme at 37ºC for 15 minutes in a vertical shaker, followed by washing and plating the cells in Matrigel as described above. To generate human apical-out organoids and induce polarity switching, we enzymatically removed the Matrigel surrounding the mature organoids. After this, the organoids were kept in suspension culture for at least 48 hours, during which time the conventional apical-in organoids transitioned to an apical-out orientation. This process is shown in detail in **Figure 3**.

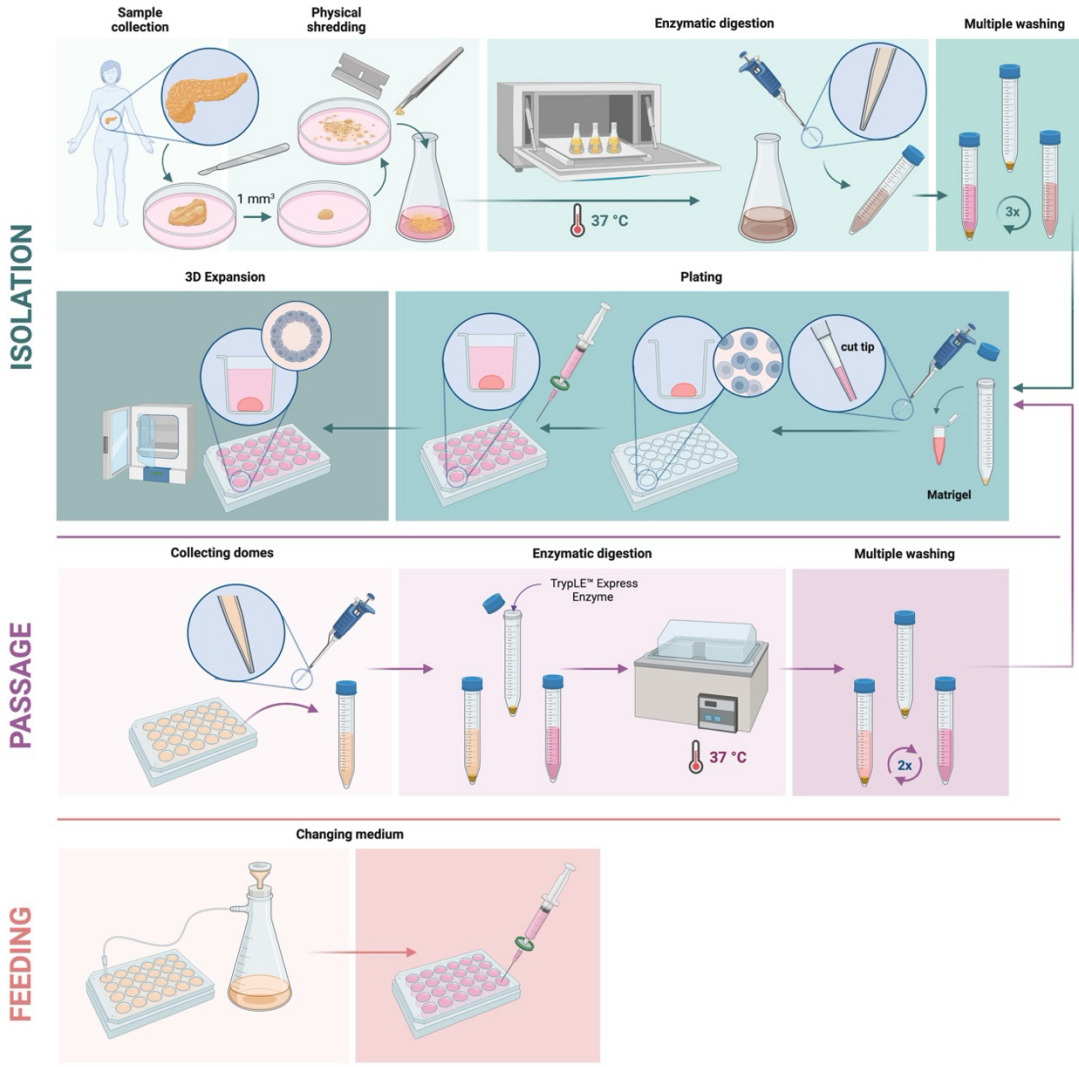

Figure 3. Workflow of human pancreatic ductal organoids generation and maintenance. **Isolation**: Workflow describing how tissues are processed to be seeded into Matrigel domes to generate PDO cultures. The tissues minced into small pieces, and ductal cells are isolated by tissue dissociation. Finally, after the washing steps the cells are resuspended in Matrigel for subsequent dome formation. Then added Feeding medium. **Passage**: Workflow describing PDOs subculturing. Organoids are digested to single cells or small fragments. The cells/fragments are seeded back in Matrigel domes to achieve PDOs expansion. **Feeding**: Workflow describing how to change the Feeding medium on the Matrigel domes. The explanatory image was created with BioRender.

7.4. Constructs, transfection, site-directed mutagenesis and gene knockdown

Plasmid DNA constructs were provided by Shmuel Muallem, Julie Forman-Kay and purchased from ORIGENE or Addgene. Transient transfections were carried out by Lipofectamine 2000 reagent. For site-directed mutagenesis Q5 high-fidelity, thermostable DNA polymerase was applied. For the gene knockdown isolated mouse ductal fragments were transfected with 50 nM siRNA or siGLOGreen transfection indicator and Lipofectamine 2000 in Feeding media for 24h. Pre-designed and validated siRNA sets used for gene-specific knockdown. A common concern with experiments derived from heterologous expression of multiple proteins is the altered endogenous stoichiometry of the proteins. To compensate for this, we performed a high number of experiments to buffer and reduce outliers, and we tried to confirm the crucial results in primary cells expressing endogenous proteins without overexpression.

7.5. End-point and qRT-PCR analysis

Total mRNA was isolated from mouse pancreatic ductal fragments by NucleoSpin RNA XS kit according to the manufacturer's instructions. The mRNA concentrations were measured by NanoDrop™ One/OneC Microvolume UV-Vis Spectrophotometer. 1 μg purified mRNA was used for the cDNA synthesis step. The efficiency of the pre-validated siRNA pools on the target genes' expression was verified at the level of mRNA by qRT-PCR. All qRT-PCR raw data was analyzed by the ΔΔCq method.

7.6. Gene expression analysis of mouse pancreatic ductal organoid cultures by RNA-Seq

RNA was extracted from the collected cell pellet separated from Matrigel described above by NucleoSpin RNA Plus kit according to the manufacturer's protocol (**Table 13.**). RNA-sequencing was performed by Illumina NextSeq 500 instrument, and data analysis process services were provided by DeltaBio2000 Ltd. Gene expression pattern was determined

according to TPM (transcript/million) values. As plasma membrane proteins display a relatively low expression levels compared to other genes, such as transcription factors, the threshold for non-expressing genes was TPM<1. The TPM values of the human CFTR gene was published previously (66).

7.7. Immunofluorescent labeling for confocal microscopy

Immunofluorescent labeling on sectioned ductal fragments was also performed on organoids as previously described (59). Briefly, sample fixation step by 4% PFA-PBS solution was always followed by washing and antigen retrieval. Sections were then blocked with BSA solution and labelled with primary and secondary antibodies against the target proteins. Images were captured by a Zeiss LSM880 confocal microscope.

7.8. Western blot and Cell Surface Biotinylation

HeLa cells were transfected with ORAI1, STIM1, and SPCA2-carrying constructs. After 18 h, cells were washed with 1X DPBS, collected with a cell scraper, and lysed with RIPA buffer supplemented with protease inhibitors. Protein electrophoresis was carried out in 10% acrylamide gels, and, after blotting, the primary antibodies were used at the following dilutions: anti-GAPDH 1:10000; anti-HA 1:1000. Secondary peroxidase-conjugated antibody was used at a dilution of 1:10000. For cell surface protein measurements PierceTM Cell Surface Biotinylation and Isolation Kit were applied according to the attached protocol. Blot picture analysis and quantification were computed by ImageJ software.

7.9. Fluorescent microscopy

Fura2-AM (5 μmol/L) and MQAE (2 μmol/L) fluorescent dyes were applied for Ca^{2+} and Cl^- measurements as described earlier (59). FRET imaging and data analysis were performed with the same hardware setup extended with a motorized emission filter wheel (Olympus CMR-U-FFWO). CFP YFP ratio data derived from FRET experiments were computed, drift corrected and normalized to the initial unstimulated values.

Calculation of the basal Ca^{2+} levels and the maximal responses. For each curve read from ROI in Ca^{2+} measurements, we calculated the baseline fluorescence ratio (average of the first 20

datapoints of F340/F380 values in each ROI), which were averaged to gain information about the basal Ca^{2+} levels. The extent of the change of the F340/F380 ratio after CM5480 administration was determined and was represented as ΔF340/F380. Correction for bleaching due to the chemical properties of the dyes during the fluorescent microscopy was compensated by drift correction for all curves (and all type of experiments) throughout the data analysis. Leak and bleaching were determined using untreated cells. Each ROIs represent one experiment and the number of samples of different experiments is shown in the bar chart.

7.10. *In vitro* and *in vivo* measurement of pancreatic fluid secretion

Isolated pancreatic ductal fragments were attached to poly-L-lysine coated cover glasses and perfused with HEPES or HCO_3^--buffered solutions at 37°C. Changes in intraluminal volume were monitored by transmitted video microscopy with Olympus IX73 inverted microscope. The relative intraluminal volume was evaluated with Scion Image software as described earlier (71). For *in vivo* pancreatic fluid secretion measurements CM5480 (i.p.; 20 mg/bwkg) or vehicle was administered twice every 24 hours before *in vivo* pancreatic fluid collection (72). Mice were anaesthetized and injected with secretin (0.75 clinical unit/bwkg, i.p.) and the pancreatic juice was collected for 30 min. The secretory rate was calculated as µl/body weight (in g)/1 h.

7.11. Direct Stochastic Optical Reconstruction Microscopy (dSTORM)

Samples labelled with immunofluorescent technique were immersed in glucose oxidase and catalase containing blinking buffer solution. dSTORM images were captured by Nanoimager S (Oxford Nanoimaging ONI Ltd.).

Definition of co-clusters. According to the geometry of the ER-plasma membrane junctions these membrane contact sites are generally under 300 nm in length in linear profiles (73). Therefore, we determined the criteria for co-localisation clusters with a maximal size of 300 nanometers. The co-clusters were quantified as histograms that indicate information about the blinking frequency and distance of a representative cluster - which is also presented in the image format - showing colocalization of the two proteins of interest within 300 nm. The pie charts show the proportion of clusters, defined as colocalization clusters, within the threshold value as a function of all clusters that have recorded blinking events from only one of these proteins within 300 nm of the cluster centromere.

7.12. FLIM-FRET measurements

GFP or YFP (donor) and mCherry (acceptor) tagged protein constructs were used during the experiments. Fluorescence lifetime (FLIM) measurements were performed using a PicoQuant LSM upgrade kit installed into a Nikon C2+ confocal unit. A special beam splitter unit was designed to easily switch between TCSPC-based FLIM and traditional confocal modes. The donor lifetimes were measured in the 520/35 emission channel in the presence of the acceptor. Then, after acceptor bleaching with a 561 nm wavelength CW laser, donor lifetime was also measure in the absence of the acceptor. FRET efficiency was calculated for each cell based on the changes in the average donor lifetime ($E = 1 - \frac{\tau DA}{\tau D}$)

7.13. Statistical analysis

All data are expressed as means ± SEM. Shapiro-Wilk normality test was applied. Both parametric (Unpaired t-test or one-way analysis of variance with Tukey's multiple comparisons test) and nonparametric (Mann-Whitney test and Kruskal-Wallis test) tests were used based on the normality of data distribution. P value below 0.05 was considered statistically significant. All statistical analyses were carried out by GraphPad Prism software (Version 8.3.1.).

8. RESULTS

8.1. ORAI1-mediated extracellular Ca^{2+} entry is constitutively active in primary polarized epithelial cells

To establish the role of SOCE in secretory epithelial cells, we first determined the expression of key signalling components using RNA sequencing of human and mouse pancreatic ductal organoids. Transcriptome analysis, confirmed by endpoint PCR, revealed expression of all 3 Orai family members (Orai1/2/3), the ER Ca^{2+} sensors Stim1 and Stim2 and the regulator protein Saraf **(Figure 4.)**.

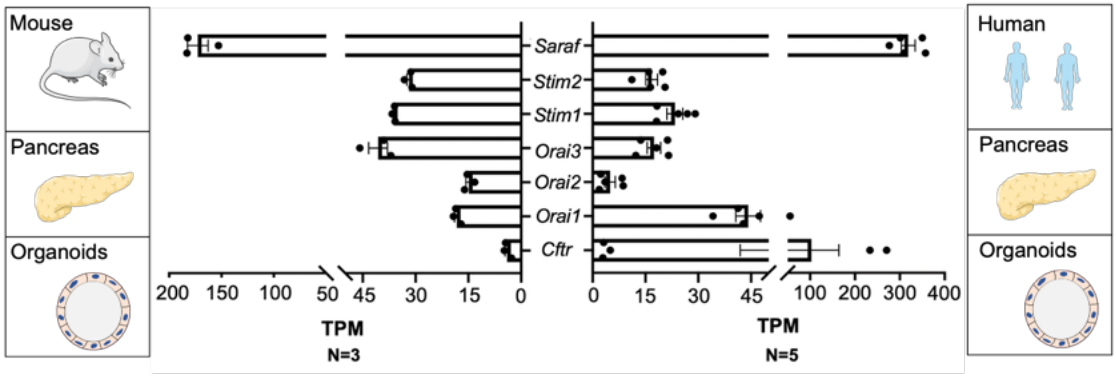

Figure 4. Expression level of SOCE-related genes in mouse (n = 3) and human (n= 5) pancreas organoids. All data are given in TPM (transcript/million). The TPM values of the human CFTR gene were published previously (66).

ORAI1 was primarily localized on the apical PM with a low level in the basolateral membrane of pancreatic ductal cells, as demonstrated in cross-sections of mouse isolated ductal fragments **(Figure 5.)**.

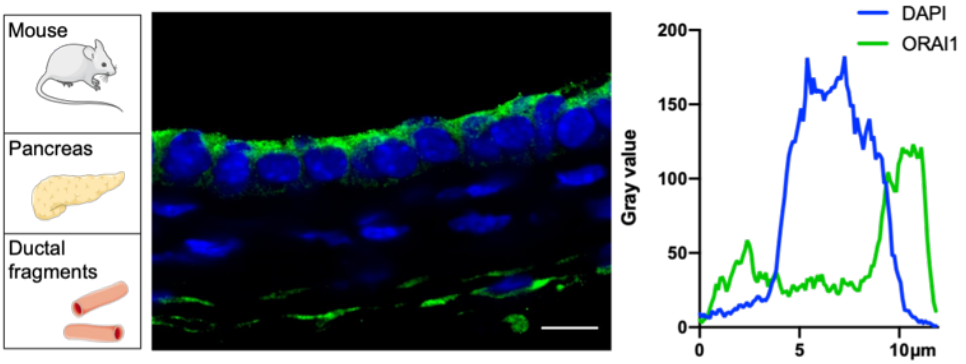

Figure 5. Representative confocal image and line profile analysis of ORAI1 protein in primary isolated pancreatic ductal fragments (scale bar: 10 µm).

Interestingly, administration of the selective ORAI1 inhibitor CM5480 in the presence of 1 mM extracellular Ca^{2+} to mouse isolated ductal fragments markedly reduced the intracellular Ca^{2+} concentration ($[Ca^{2+}]_i$) of epithelial cells without prior ER Ca^{2+} store depletion **(Figure 6/A.)**. On the other hand, removing the extracellular Ca^{2+} triggered a marked drop of $[Ca^{2+}]_i$, which was not further decreased by CM5480 **(Figure 6/B.)**. CM5480 significantly impaired the $[Ca^{2+}]_i$ increase in response to carbachol stimulation when administered during the plateau phase of the signal in ductal fragments **(Figure 6/C.)**. To rule out that the ER Ca^{2+} stores were artificially depleted, we directly measured the ER Ca^{2+} store content by transfecting the primary epithelial cells in human pancreatic apical-out organoids with the genetically encoded Ca^{2+} sensor pcDNA3-D1ER (66,74). We detected a rapid decrease in the D1ER fluorescence resonance energy transfer (FRET) ratio upon ER store depletion with 10 µM cyclopiazonic acid (CPA) **(Figure 6/D.)**.

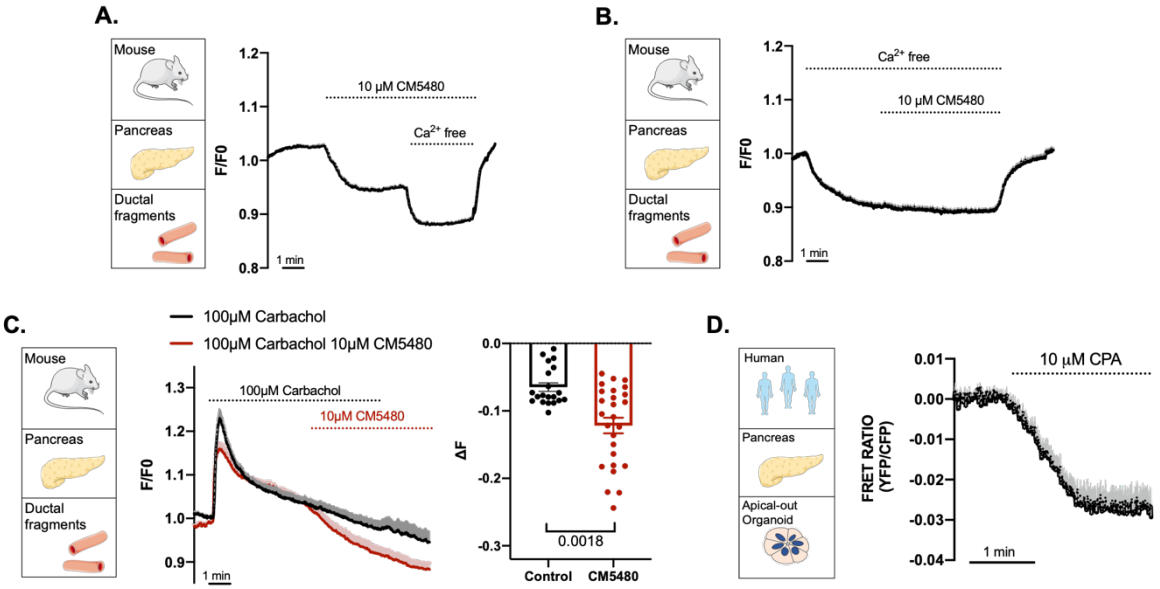

Figure 6. A. Intracellular Ca^{2+} levels were monitored using Fura 2-AM in unstimulated murine ductal fragments where treatment with 10 µM CM5480, a pharmacological inhibitor of ORAI1, resulted in a marked decrease in basal Ca^{2+} levels. **B.** Removal of extracellular Ca^{2+} resulted in a decreased intracellular Ca^{2+} level in isolated ductal fragments, which was not reduced further by subsequent treatment with 10 µM CM5480. **C.** 100 µM carbachol was applied to induce a peak-plateau Ca^{2+} signal. The administration of 10 µM CM5480 disrupted the plateau phase of the signal as demonstrated by average traces and bar chart. **D.** Average traces of 3 individual FRET experiments after D1ER sensor transfection into apical-out human pancreatic organoids demonstrate that the Ca^{2+} stores are not depleted, as indicated by the decreasing FRET ratio (YFP/CFP) in response to 10 µM CPA.

Importantly, gene knockdown by siOrai1 and siStim1 abolished the response to CM5480 in the primary ductal cells and reduced the basal $[Ca^{2+}]_i$ that was significantly impaired in both cases, compared with the siGLO green transfected controls **(Figure 7.)**.

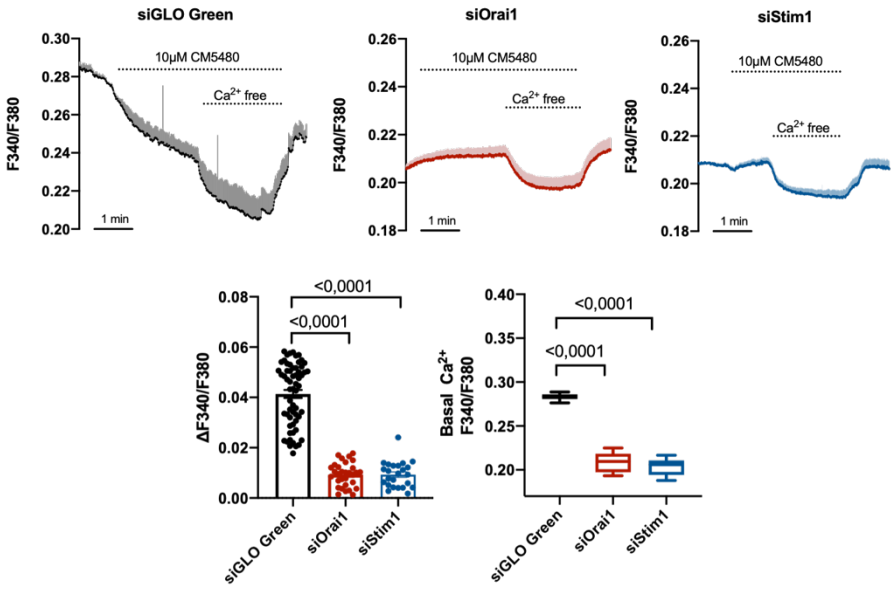

Figure 7. The effect of 10 μM CM5480 was abolished by siOrai1 and siSim1 treatment. The same genetic perturbations decreased the basal Ca^{2+} level significantly.

The residual reduction in $[Ca^{2+}]_i$ in response to extracellular Ca^{2+} removal was retained in siStim1- and siOrai1-treated cells. To test if constitutive ORAI1 activity is specific to pancreatic cells or common among secretory epithelia, we generated airway and liver organoids from mice and pancreatic organoids from human cadaver donors. In unstimulated mouse lung **(Figure 8/A.)** and liver **(Figure 8/B.)** and in human pancreatic organoids **(Figure 8/C.)**, the inhibition of ORAI1 with 10 μM CM5480 resulted in a prominent decrease of $[Ca^{2+}]_i$. These experiments revealed that the ORAI1-mediated extracellular Ca^{2+} influx is constitutively active in primary mouse and human secretory epithelial cells that significantly contribute to the maintenance of basal $[Ca^{2+}]_i$.

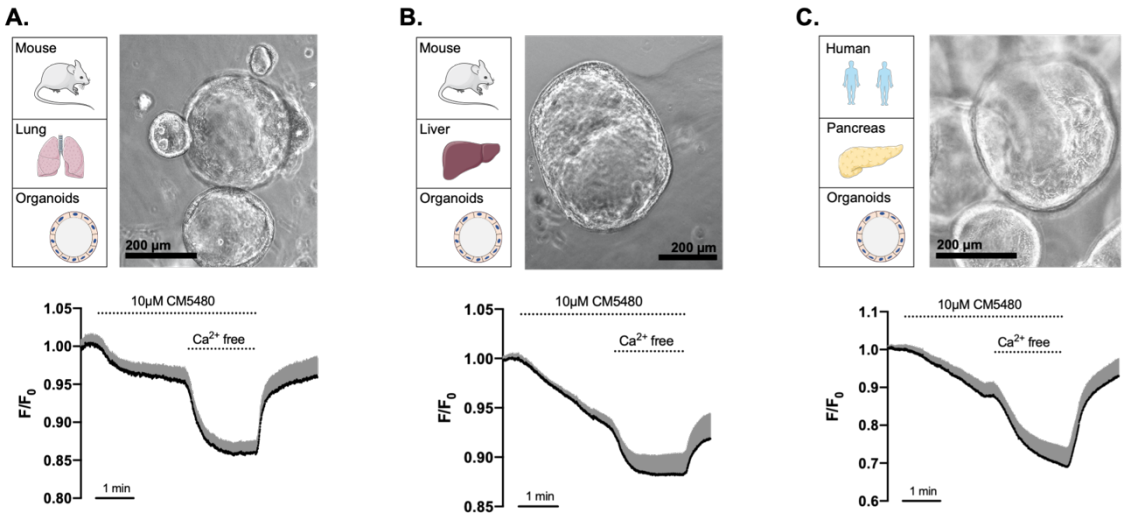

Figure 8. A-C. Average traces of 3–5 experiments are demonstrated in each indicated Ca^{2+} measurement. Transmitted light microscopy images of cystic organoids in mouse lung **(A)**, mouse liver **(B)**, and human pancreatic cultures **(C)**. ORAI1 inhibition significantly decreased the resting intracellular Ca^{2+} level in mouse lung **(A)**, mouse liver **(B)**, and human pancreatic organoid cultures (OCs) **(C)**. Average traces of 3–4 experiments were carried out on each biological sample types.

8.2. SPCA2 maintains constitutive ORAI1 activity in primary epithelial cells

In the next step, we examined the whole transcriptome of mouse and human pancreatic organoids for unbiased analysis of the potential regulatory components that maintain the constitutive activity of ORAI1. The sequencing identified transcripts of several STIM1/ORAI1-interacting proteins in pancreatic organoids, and among these, three different store-independent regulators – *Spca1-2* (also known as Atp2c1-2) and *Septin7* – were determined **(Figure 9.)**.

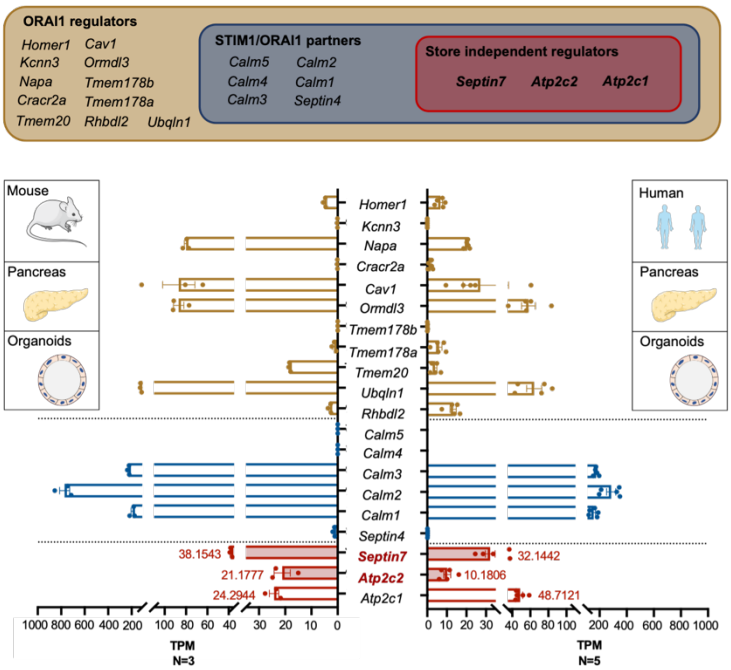

Figure 9. Expression profile of ORAI1 regulators (brown), STIM1/ORAI1 interacting partners (blue), and store-independent ORAI1 regulators (red) in mouse (n = 3) and human (n = 5) pancreas OCs.

A previous study described a possible role of SPCA2 – a member of the SPCA family – in a store-independent ORAI1-mediated Ca^{2+} entry in breast cancer cells. SEPTIN7 emerged as a potential store-independent negative modulator of part of the extracellular Ca^{2+} influx. Of note, previous studies identified a pancreatic acinar cell-specific isoform of SPCA2 (termed SPCA2C), which was not found in pancreatic ductal cells. According to the Human Proteome Atlas, pancreatic ductal cells express the full-length SPCA2. In addition, previous studies suggested that both the N′- and C′-terminal domains of SPCA2 have important functions in the protein-protein interactions. Therefore, in this study, we focused on the full-length SPCA2. To

test the role of these proteins in primary epithelial cells, we treated mouse ductal fragments with small interfering RNA (siRNA), for Spca1, 2, and Septin7, and measured the changes in $[Ca^{2+}]_i$. In these series of experiments, siSPCA2 treatment lowered the basal $[Ca^{2+}]_i$ and significantly decreased the constitutive ORAI1-mediated extracellular Ca^{2+} influx in unstimulated mouse primary ductal epithelial cells, whereas siSPCA1 or siSEPT7 has no effect when compared with the siGLO green transfected control (**Figure 10.**).

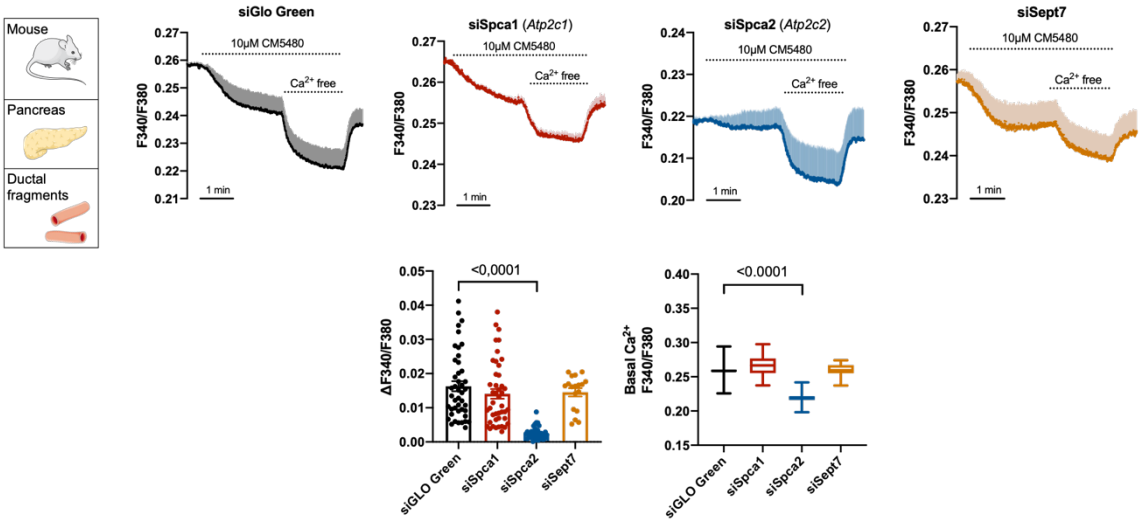

Figure 10. Average traces and plots show the effect of siRNA perturbation (Spca1, Spca2, Sept7) on the resting intracellular Ca^{2+} level in mouse pancreatic ductal fragments.

To understand the role of SPCA2 in the regulation of ORAI1, we analyzed the intracellular distribution of SPCA2 and ORAI1 in transiently transfected HeLa cells. In these cells, ORAI1 showed partial puncta formation, whereas SPCA2 showed a reticular ER-like expression pattern in unstimulated cells (**Figure 11/A.**). Notably, this expression pattern was not changed by the depletion of the ER Ca^{2+} stores with 10 μM CPA.

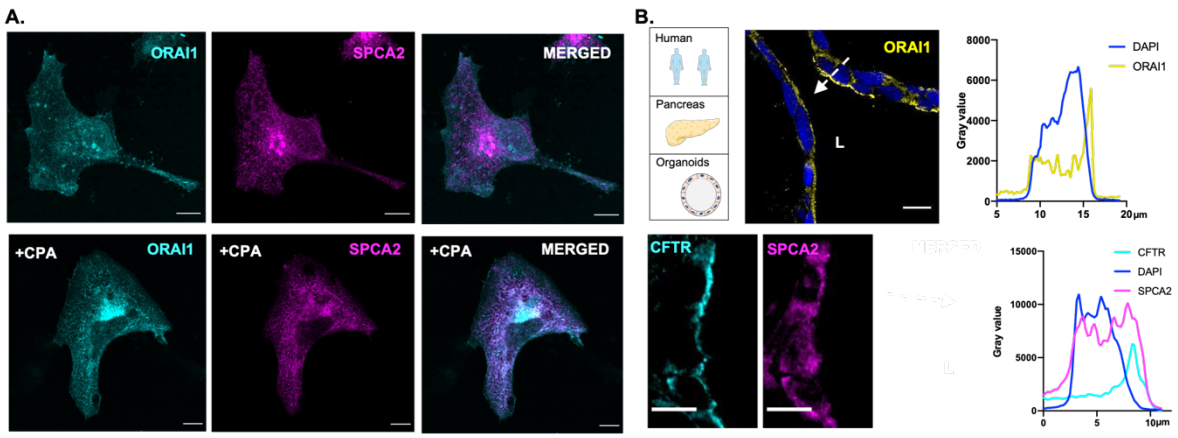

Figure 11. A. Representative confocal image demonstrates the localization and distribution of ORAI1 and SPCA2 in co-transfected HeLa cells with and without 10 µM CPA treatment (white color represents the overlapping areas). **B.** Representative confocal image and line profile analysis demonstrate the localization of ORAI1 and of CFTR and SPCA2 in human pancreatic organoids (scale bar: 10 µm; L, luminal/apical side).

Owing to antibody incompatibility, the co-staining of ORAI1 and SPCA2 was not possible, therefore CFTR Cl^- channel was used as an apical membrane marker (**Figure 11/B.**).

To further assess the co-localization of ORAI1 and SPCA2, we used super-resolution microscopy. Direct Stochastic Optical Reconstruction Microscopy (dSTORM) images confirmed partial co-localization of the SPCA2-ORAI1 clusters in resting and stimulated cells as well **(Figure 12/A.)**.

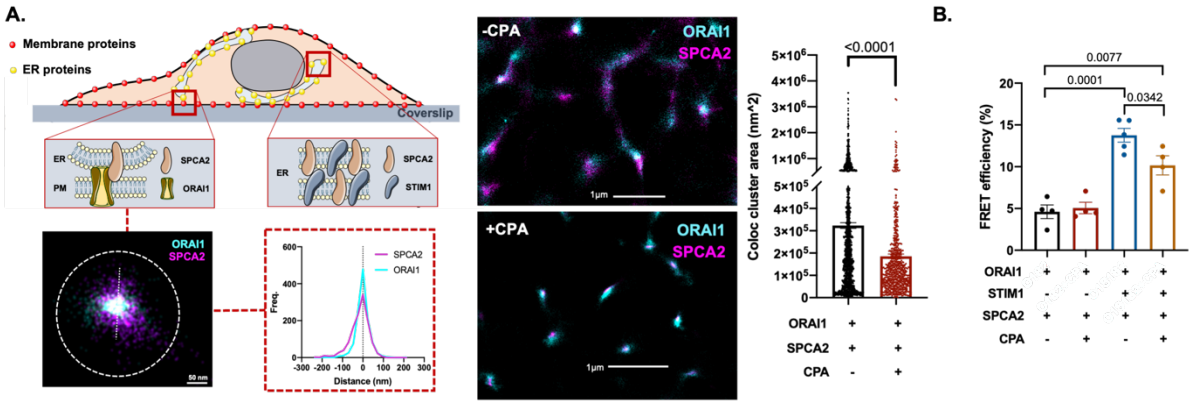

Figure 12. A. Schematic figure, dSTORM images and histogram demonstrate the physical proximity of ORAI1-SPCA2 in the focal plane of the PM. Super-resolution images and high-throughput cluster analysis show significantly decreased cluster area values upon 10 µM CPA treatment. **B.** The calculated FRET efficiency from FLIM measurements between ORAI1 and SPCA2 is presented in a bar chart.

Of note, the clusters of SPCA2 displayed a reticular expression pattern, whereas ORAI1 clusters were more compact in unstimulated cells. In cells stimulated with 10 µM CPA, the co-cluster area significantly decreased. The criteria for co-clusters were deafened based on the extent of the ER-PM contact sites. Clusters of two proteins of interest were counted as co-clusters if the individual clusters were located within a maximal size of 300 nm. This observation was further investigated by fluorescent lifetime measurement (FLIM) based on the determination of FRET efficiency using SPCA-GFP (donor) and ORAI1-mCherry (acceptor). These experiments revealed that SPCA2 and ORAI1 are in physical proximity in unstimulated cells (FRET efficiency: 4,61%), which was not increased further by CPA stimulation **(Figure 12/B.)**. In contrast, the presence of STIM1 was sufficient to remarkably increase the FRET between ORAI1 and SPCA2, which was again not increased further by CPA stimulation. In the latter case, we even detected a moderate decrease in the FRET, which could be explained by the

competition of STIM1 with SPCA2 for the binding sites of ORAI1. As SPCA2 does not participate in SOCE, it is not unexpected that CPA stimulation does not increase the SPCA2-ORAI1 interaction. Expression of ORAI1 and SPCA2 generated a constitutively active Ca^{2+} influx, which was not affected by the SPCA2 mutants **(Figure 13.)**. These results suggest that SPCA2 regulates the SICE via ORAI1 independently from SPCA2 Ca^{2+} influx in epithelial cells.

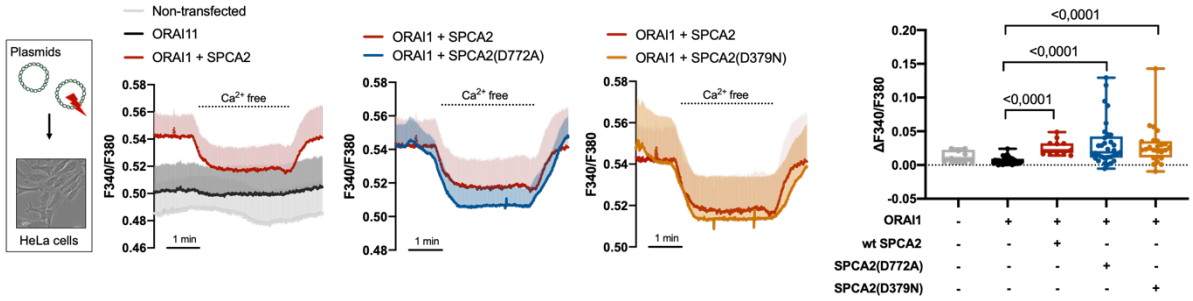

Figure 13. HeLa cells were transfected with wild-type ORAI1 and wild-type or mutant (D772A or D379N) SPCA2-carrying plasmids. Average traces and bar charts demonstrate that ORAI1 alone resulted in lower basal Ca^{2+} levels compared with co-transfected cells. None of the introduced SPCA2 mutations altered the significantly increased basal Ca^{2+} levels and Ca^{2+} influx caused by the co-transfection. Average traces of 3–4 experiments are demonstrated in each indicated measurement.

8.3. SPCA2 increases the interaction between STIM1 and ORAI1

Our data indicate that SPCA2 can activate ORAI1-mediated, store-independent extracellular Ca^{2+} entry; however, the findings also point to the involvement of STIM1 in this process. Therefore, we wanted to understand how SPCA2 affects STIM1-ORAI1 interactions. In unstimulated HeLa cells, the overexpressed SPCA2 and STIM1 showed a reticular ER expression pattern **(Figure 14/A.)**, and STIM1 showed a significant punctation. To gain higher spatial resolution, we used dSTORM, which revealed that STIM1 and SPCA2 overlapped in the focal plane of the ER **(Figure 14/B.)**. The SPCA2-induced puncta formation of ORAI1 was further quantified in STIM1-ORAI1 co-transfected cells. In the absence of Ca^{2+} store depletion, only a minimal number of STIM1/ORAI1 co-clusters were observed **(Figure 14/C.)**. Co-transfection of ORAI1-STIM1 with SPCA2 resulted in a profound increase in spontaneous puncta formation in cells with filled Ca^{2+} stores, which was further increased by store depletion. To quantify STIM1-ORAI1 cluster overlap with and without SPCA2, using dSTORM, we co-transfected cells with STIM1 and ORAI1 ± SPCA2. Without ER Ca^{2+} store depletion, STIM1-ORAI1 co-localization was negligible but markedly increased after CPA-induced store depletion **(Figure 14/D.)**.

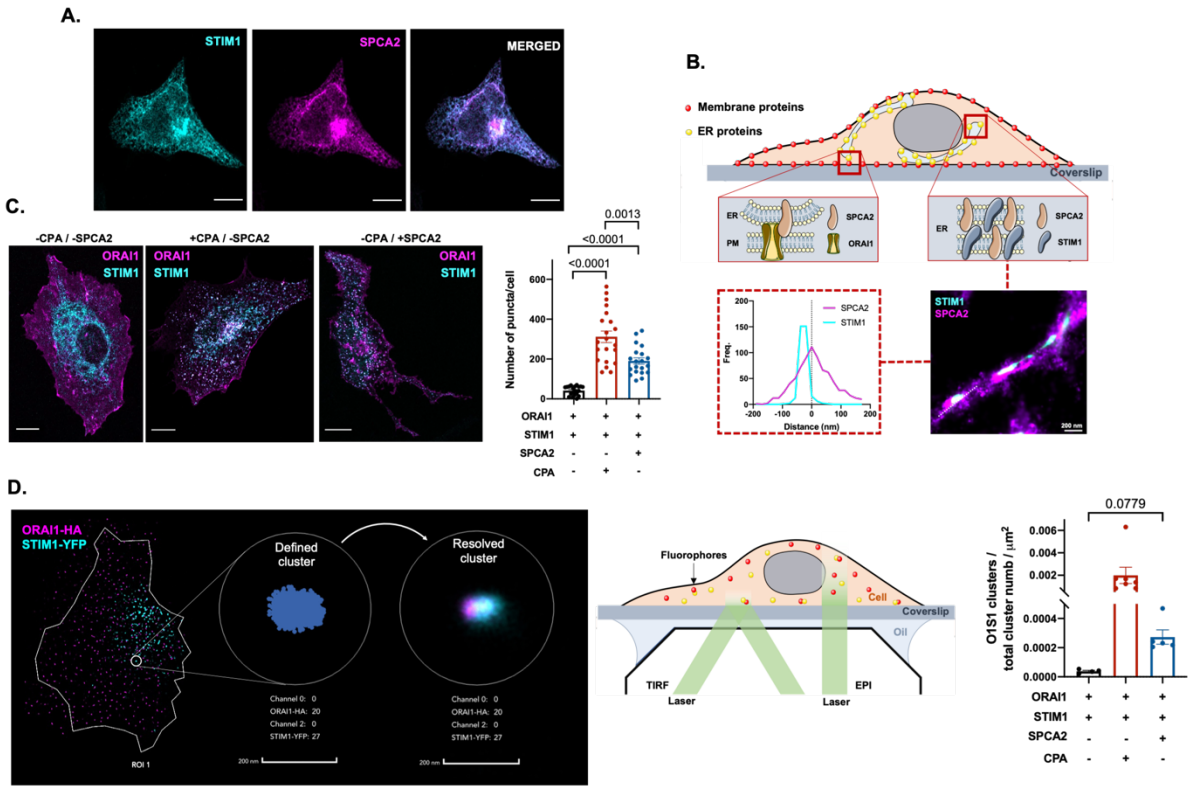

Figure 14. A. Confocal pictures demonstrate the intracellular co-localizing distribution of the reticular STIM1 and SPCA2 proteins in co-transfected HeLa cells (scale bar: 10 µm). **B.** Schematic figure and dSTORM images demonstrate the physical proximity of ORAI1-SPCA2 in the ER membrane. The frequency of blinking events was plotted as a function of the distance from the indicated white dashed lines. **C.** Confocal images and bar chart demonstrate significant differences in puncta formation between the three indicated experimental groups (ORAI1 + STIM1, ORAI1 + STIM1 + 10 µM CPA, ORAI1 + STIM1 + SPCA2). **D.** Schematic illustration of the dSTORM cluster analysis and experimental setup using total internal reflection fluorescence (TIRF) resulted in the determination of the ORAI1-STIM1 co-localizing cluster ratio in the focal plane of the PM. The bar chart shows the maximum number of ORAI1-STIM1 co-localizing clusters normalized to µm^2 membrane area.

Importantly, SPCA2 significantly increased the number of STIM1-ORAI1 co-clusters in cells with filled stores. This observation was further investigated by FLIM-FRET, using STIM1-YFP (yellow fluorescent protein) (donor) and ORAI1-mCherry (acceptor). The calculated FRET efficiency was significantly increased by SPCA2, compared with the group without SPCA2 transfection (**Figure 15/A.**). As expected, CPA treatment further increased FRET efficiency. The constitutive Ca^{2+} influx and increased STIM1-ORAI1 clustering may be caused by enhanced Ca^{2+} leakage and reduced ER Ca^{2+} stores in SPCA2-expressing cells. To exclude the possibility that STIM1-ORAI1 clustering is caused by the leakage of the ER Ca^{2+} stores, we measured the ER Ca^{2+} store content in HeLa cells transfected with D1ER and treated with 10 µM CPA. These experiments showed no effect of SPCA2 on the ER Ca^{2+} content (**Figure 15/B.**).

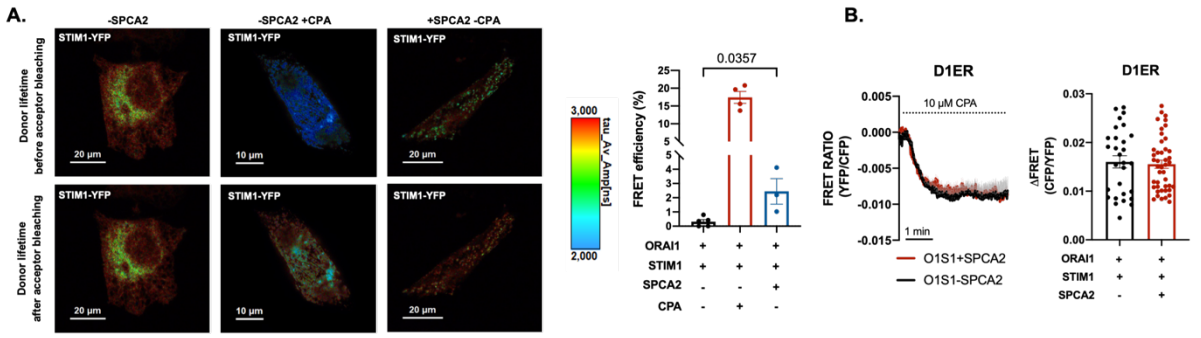

Figure 15. A. Confocal images and the calculated FRET efficiency between Stim1-YFP (donor) and ORAI1-mCherry (acceptor) plotted on a bar chart of the FLIM measurements. **B.** Average traces of 3–4 FRET experiments demonstrate no significant difference upon 10 µM CPA treatment in Ca^{2+} extrusion from the ER in the presence or absence of SPCA2 in STIM1-ORAI1 (O1S1) co-transfected HeLa cells by using D1ER FRET sensor.

A previous study suggested that SPCA2 is required for the PM trafficking of ORAI1. Therefore, we quantified the expression of ORAI1 by western blot and cell surface biotinylation assay, which revealed that the total expression of ORAI1 is not changed significantly in the presence of SPCA2 (**Figure 16/A.**). Although, ORAI1 cell surface expression was moderately decreased in the SPCA2 transfected cells, the difference was not significant (**Figure 16/B.**). The silencing of SPCA2 in ORAI1-overexpressing HeLa cells had no significant effect on ORAI1 surface levels, as revealed by capillary western blotting (**Figure 16/B.**). To further validate the proposed complex, we performed co-immunoprecipitation (coIP) using hemagglutinin (HA)-tagged ORAI1 in HeLa cells co-expressing STIM1-GFP and SPCA2-Myc. Both STIM1 and SPCA2 were detected in the HA pull-down fraction (**Figure 16/C.**), confirming their biochemical association with ORAI1. Notably, the increased basal STIM1-ORAI1 clustering by SPCA2 in the absence of apparent ER Ca^{2+} depletion that could not be observed when STIM1 and SPCA2 were co-expressed in the absence of ORAI1 suggest that SPCA2 acts on ORAI1 first, and when clustering ORAI1, it stabilized clustering of STIM1, as it is known that ORAI1 reduces STIM1 mobility to stabilize STIM1 clustering. However, for the constitutive Ca^{2+} influx, the presence of STIM1 in the complex is also crucial.

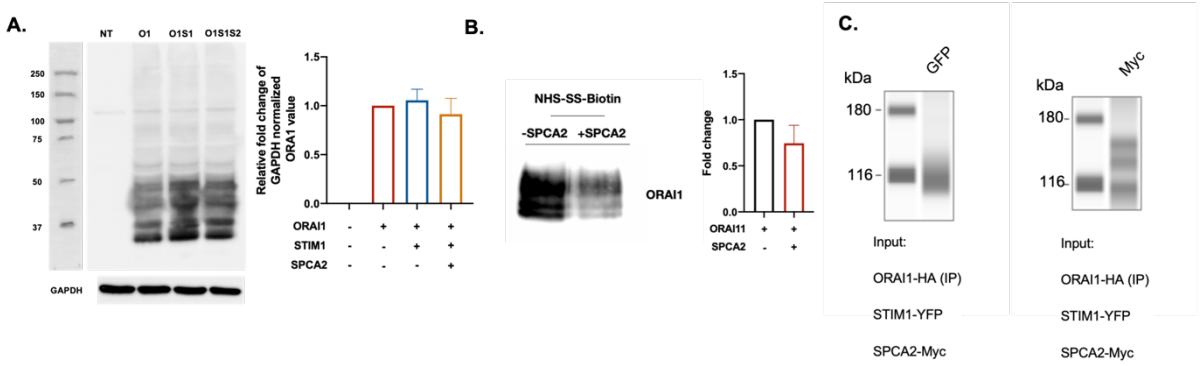

Figure 16. A. Western blot shows no change of the expression of ORAI1 (normalized to GAPDH intensity) in whole-cell lysate with STIM1 (O1S1) and STIM1-SPCA2 (O1S1S2) co-transfected cells (n = 3). **B.** Cell surface expression of ORAI1 was not changed significantly in SPCA2 co-transfected cells compared with control (n = 2). **C.** Western blot analysis of the coIP eluates revealed the presence of STIM1-YFP (left, anti-GFP) and SPCA2-Myc (right, anti-Myc) in the immunoprecipitated complex, confirming their association with ORAI1. Molecular weight markers are shown in kDa. Input constructs are indicated below.

8.4. ORAI1-mediated SICE regulates CFTR activity and fluid secretion in pancreatic ductal epithelial cells

The physiological role of spontaneous Ca^{2+} influx activated by SPCA2 via ORAI1 is unknown. We investigated whether it regulates epithelial ion and fluid secretion, mediated largely by the CFTR Cl^- channel. Thus, we first clearly demonstrated CFTR and ORAI1 co-localization on the apical membrane of mouse pancreatic ductal organoids (**Figure 17.**).

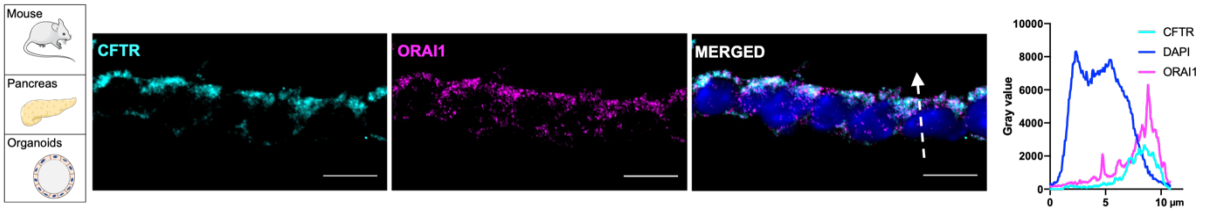

Figure 17. Confocal pictures and line profiles demonstrate the co-localization of CFTR and ORAI1 at the apical membrane of mouse pancreatic organoids (Pearson's coefficients: r = 0.857) (scale bar: 10 µm).

The CFTR-ORAI1 co-localization was further confirmed by capturing dSTORM images of transfected HeLa cells and 2D adherent primary ductal cells generated from human pancreatic organoids, which endogenously expressed the two proteins (**Figure 18.A/B.**)

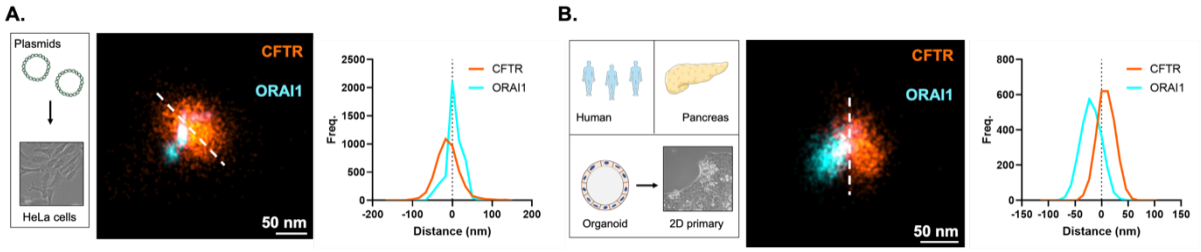

Figure 18. A. Evaluated representative dSTORM picture illustrates the physical proximity of CFTR and ORAI1 in the PM of co-transfected HeLa cells and adherent culture derived from human pancreatic organoids. **B.** The frequency of blinking events was plotted as a function of the distance from the indicated white dashed lines **(A and B)**.

The combined localization *ex vivo* and dSTORM analysis suggest that CFTR and ORAI1 are located in the same PM nanodomain. To examine the role of SICE in CFTR activity, we measured CFTR-mediated Cl^- extrusion in pancreatic ductal fragments using the Cl^- - sensitive

dye MQAE (N-(Ethoxycarbonylmethyl)-6-Methoxyquinolinium Bromide), whose fluorescence increases upon Cl^- efflux. Removal of extracellular Cl^- from the HCO_3^-/CO_2-buffered solution resulted in a decrease in $[Cl^-]_i$, which was abolished by 10 µM of the selective CFTR inhibitor CFTR(inh)-172 (**Figure 19/A.**). Notably, treating the ductal cells with 10 µM CM5480 or pre-incubation with 40 µM BAPTA-AM (1,2-bis(o-aminophenoxy) ethane-N, N, N', N'- tetraacetic acid) to chelate and buffer $[Ca^{2+}]_i$ resulted in a similar inhibition of Cl^- efflux (**Figure 19/A.**). Moreover, the knockdown of ORAI1 or STIM1 with siRNA resulted in a marked decrease in the Cl^- efflux (**Figure 19/B.**). On the other hand, the higher forskolin-stimulated maximal CFTR Cl^- efflux was not affected by the inhibition of ORAI1 with CM5480, suggesting that the stimulated secretion is independent of SICE (**Figure 19/C.**). These findings indicate that the spontaneous ORAI1-mediated SICE has a specific and major impact on the basal CFTR activity in ductal epithelial cells.

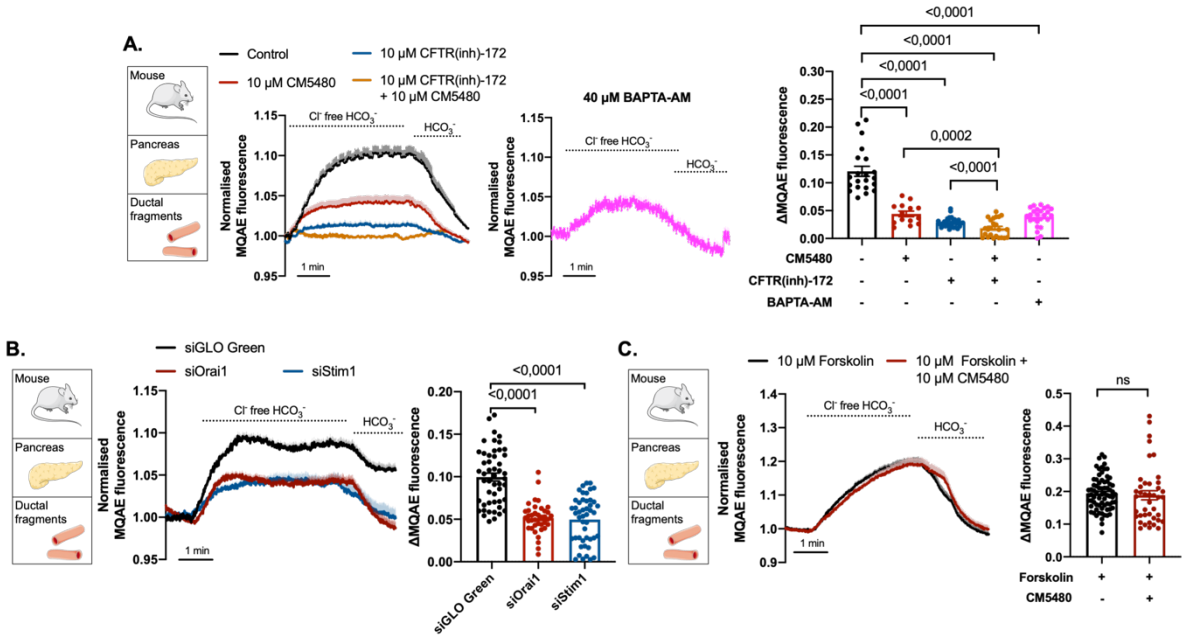

Figure 19. A. The intracellular Cl^- level was measured by MQAE in pancreatic ductal fragments where the quantity of intracellular Cl^- and the intensity of fluorescence are inversely proportional. Challenging the cells with Cl^--free extracellular solution resulted in a decrease in intracellular Cl^-, which was completely abolished by 10 µM CFTR(inh)-172. Inhibition of ORAI1 or global Ca^{2+} chelation with 40 µM BAPTA-AM pre-incubation significantly decreased the CFTR-mediated Cl^- efflux. The bar chart represents the maximal change of MQAE fluorescence upon extracellular Cl^- withdrawal in each investigated experimental group. **B.** Average traces of 3–4 experiments and bar chart demonstrate that Orai1 or Stim1 knockdown by siRNA significantly decreased CFTR-mediated Cl^- efflux. **C.** Forskolin-stimulated Cl^- efflux was not changed by 10 µM CM5480 in isolated pancreatic ducts.

To confirm the role of SPCA2 in regulating CFTR activity, the expression of SPCA1 and 2 and SEPTIN7 were knocked down in mouse pancreatic ductal fragments. In accord with the intracellular Ca^{2+} measurements, the activity of CFTR was significantly impaired by siSPCA2,

while siSPCA1 and siSEPT7 had no effect (**Figure 20/A.**). We assessed CFTR-dependent pancreatic ductal HCO_3^- and epithelial fluid secretion. Pancreatic ductal epithelial cells take up and extrude HCO_3^- in HCO_3^-/CO_2 buffered solution, which was significantly impaired by 10 µM CM5480 (**Figure 20/B.**). In addition, the spontaneous swelling of the untreated ductal fragments in HCO_3^-/CO_2 buffered solution was significantly impaired by ORAI1 inhibition (**Figure 20/C.**), suggesting the inhibition of the basal, unstimulated fluid secretion. Finally, to confirm our findings *in vivo*, the pancreatic fluid secretion was measured in control and CM5480-treated mice, which revealed that the inhibition of ORAI1 significantly inhibited the *in vivo* pancreatic ductal fluid secretion (**Figure 20/D.**) Our results demonstrate that SICE via the SPCA2/STIM1/ORAI1 complex determines basal CFTR activity and thus ion and fluid secretion in pancreatic ductal cells.

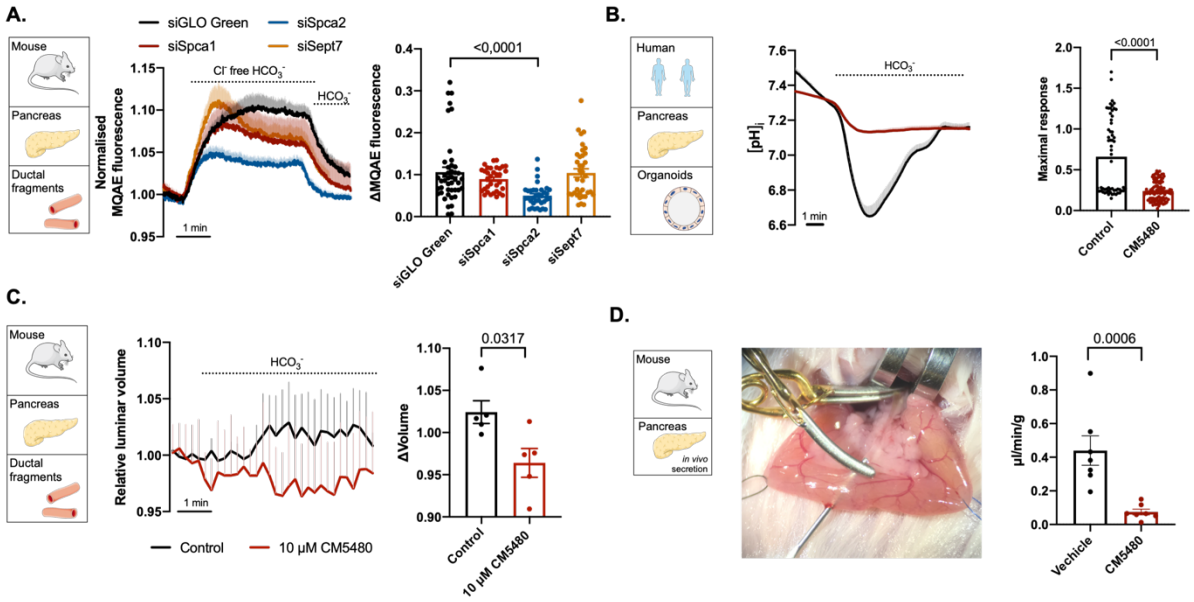

Figure 20. A. Among siSpca1, siSpca2, and siSept7, only knockdown of Spca2 resulted in significantly decreased Cl^- efflux, as represented by average traces and bar chart. **B.** Intracellular pH measurements with BCECF-AM HCO_3^- extrusion in HCO_3^-/CO_2 buffered solution was significantly impaired by 10 µM CM5480 in human pancreatic organoids. **C.** Spontaneous swelling of unstimulated ductal fragments in HCO_3^-/CO_2 buffered solution was significantly impaired by 10 µM CM5480. **D.** *In vivo* pancreatic fluid secretion was inhibited by CM5480 treatment (n = 7/group).

8.5. SICE via ORAI1 regulates CFTR activity in secretory epithelial cells

To determine whether the co-localization of ORAI1 and CFTR and the regulatory role of constitutive SICE by ORAI1 are ubiquitous features in secretory epithelia, we utilized organoids cultures from mouse airway, liver, and human pancreas. Immunofluorescent labeling in the organoids confirmed the co-localization of CFTR and ORAI1 on the apical membrane of epithelial cells (**Figures 21.A-C.**). In addition, inhibition of ORAI1 with 10 µM CM5480 in

unstimulated mouse lung (**Figure 21/A.**) and liver (**Figure 21/B.**) and human pancreatic organoids (**Figure 21/C.**) resulted in a decrease of the CFTR-mediated Cl^- efflux upon removal of extracellular Cl^-. Notably, the CFTR-mediated Cl^- efflux was almost completely abolished in airway organoids when the spontaneous Ca^{2+} influx was inhibited. The findings with various epithelia emphasize that regulating CFTR activity by SICE is a common regulatory mechanism in secretory epithelia in both mice and humans.

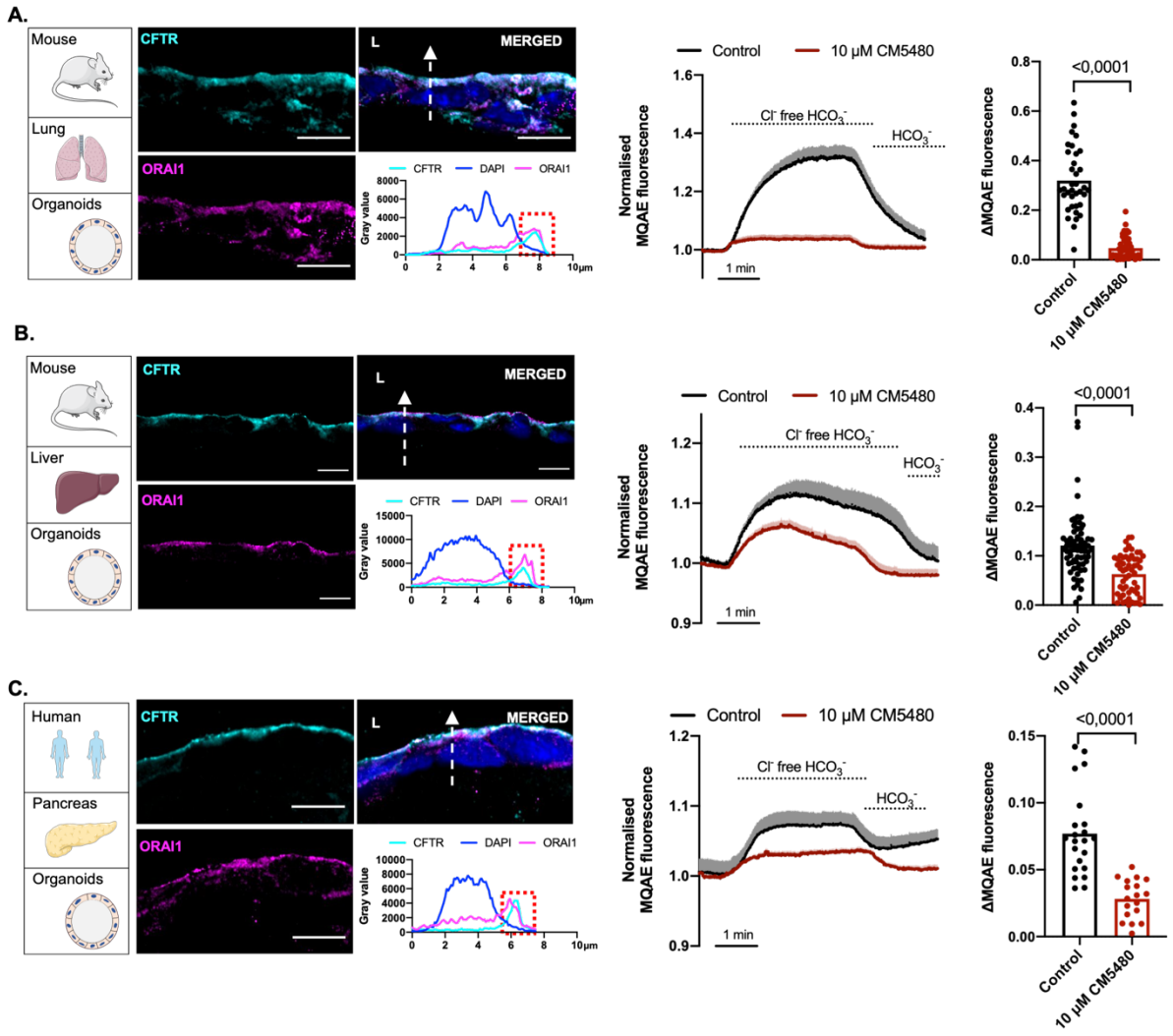

Figure 21. Confocal images and their line profile analysis demonstrate the co-localization of CFTR and ORAI1 proteins at the apical membrane of OCs derived from mouse lung **(A)**, mouse liver **(B)**, and human pancreatic tissue **(C)** (Pearson's coefficients: mouse lung-derived OC r = 0.903; mouse liver-derived OC r = 0.875; human pancreas-derived OC r = 0.688) (scale bar: 10 µm). Average traces and bar charts show that ORAI1 inhibition by 10 µM CM5480 significantly decreased CFTR activity in mouse lung **(A)**, mouse liver **(B)**, and human pancreatic OCs **(C)**.

8.6. SICE by ORAI1 regulates CFTR activity via Ca^{2+}-dependent ACs

Synergism between cAMP and Ca^{2+} signalling is a major form of regulating CFTR activity. To assess the role of SICE via ORAI1 in the regulation of local cAMP nanodomains, we first analyzed the adenyl cyclase genes (Adcy) transcriptome of the mouse and human pancreatic ductal organoids. The transcript/million (TPM) values demonstrated the expression of *Adcy3, 6, 8,* and *9* in mice with low but detectable transcript levels of *Adcy1* (**Figure 22.**).

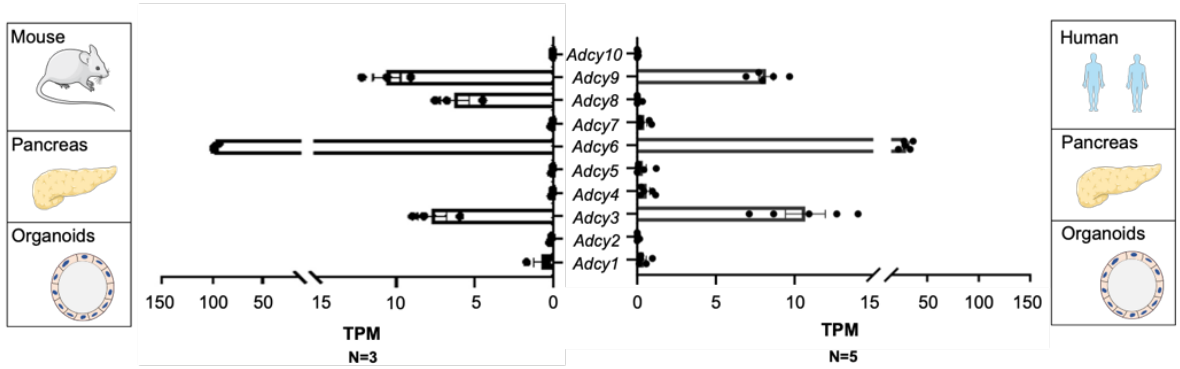

Figure 22. Expression pattern of AC family members in mouse- (n = 3) and human (n = 5) pancreas-derived OCs. All data are given in TPM values.

The dSTORM imaging of organoids was unsuccessful due to the high background noise and low signal-to-noise ratio. Therefore, we used transfected HeLa cells for the super-resolution localization of the ACs. Analysis of HeLa cells co-transfected with CFTR and AC1, AC3, AC6, or AC8, using dSTORM and cluster analysis, revealed that CFTR is in close physical proximity to AC1 (clusters overlapping: 62.04%), 3 (clusters overlapping: 34,3%), and 8 (clusters overlapping: 60.1%), with limited co-localization with AC6 (clusters overlapping: 14.56%) (**Figure 23.**).

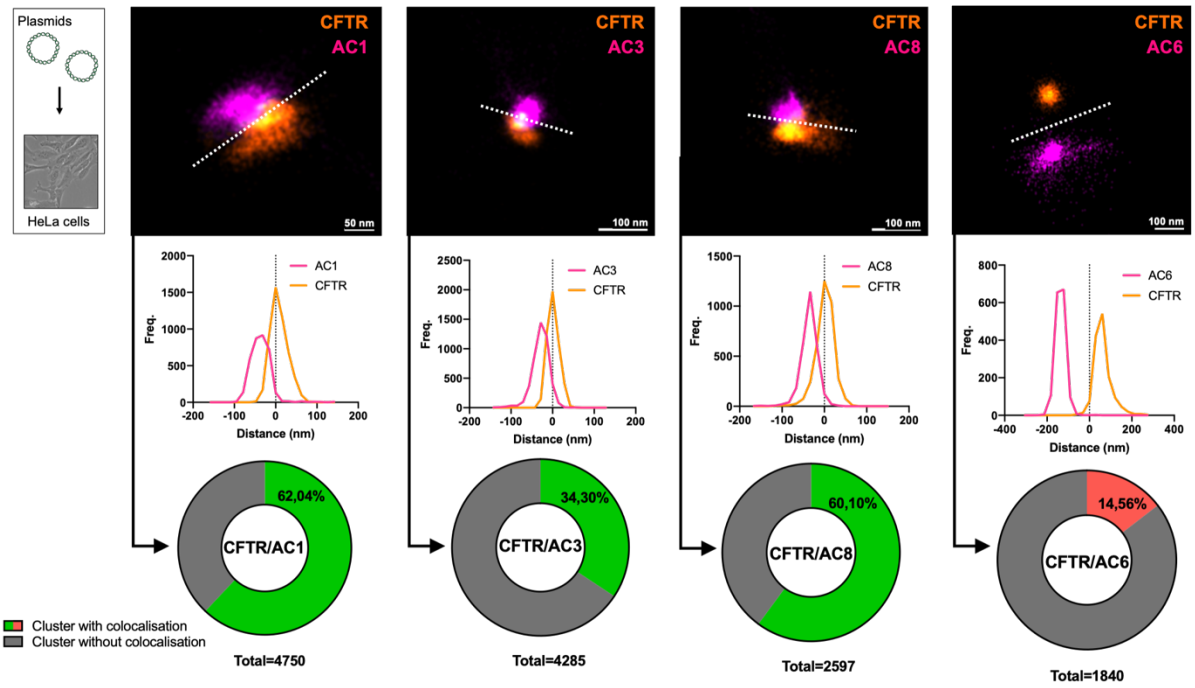

Figure 23. Representative dSTORM images show overlapping positions of CFTR and AC1/3/8/6 in the focal plane of the membrane of co-transfected HeLa cells. Cluster analysis results show the percentage of clusters with co-localizing fluorophores within a maximum radius of 300 nm from the centroids formed by individual blinking events.

In addition, these ACs co-localized with ORAI1 as well as in co-transfected HeLa cells (**Figure 24/A.**). Although AC6 is a prominent regulator of CFTR, it is inhibited by Ca^{2+} and was therefore excluded as a potential transmitter of SICE regulation to CFTR. To visualize the signalling nanodomain, we applied three-color dSTORM in HeLa cells transfected with CFTR, ORAI1, and AC1, 3, or 8, which confirmed that these three proteins are in the same PM nanodomain (**Figure 24/B.**).

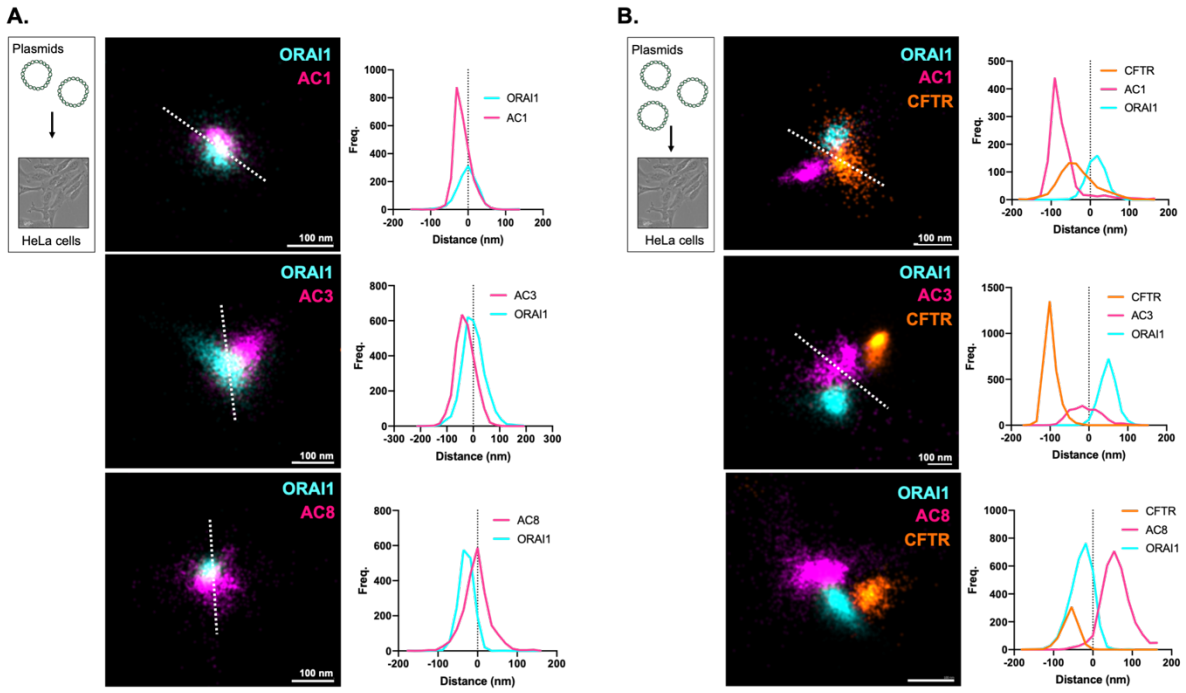

Figure 24. A. Evaluated dSTORM pictures illustrate the physical proximity of AC1/3/8 and ORAI1 in the membrane of co-transfected HeLa cells. In comparison, three-color dSTORM images demonstrate the molecular assembly of the protein nanodomain consisting of CFTR, ORAI1, and one of the AC1/3 or 8. **B.** Dashed lines indicate the zero point of the distance scale represented as a function of blinking event frequency.

Single knock-down experiments in apical-out human pancreatic organoids revealed that basal CFTR activity is most profoundly impaired upon silencing of AC8, as measured by MQAE fluorescence (**Figure 25/A.**), suggesting that AC8 is the key isoform maintaining constitutive secretion under resting conditions. Finally, we used PKA inhibitors: PKI (protein kinase inhibitor) (5-24) (100 nM; a high-affinity peptide inhibitor) and KT5720 (1 µM; a small-molecule inhibitor). Both compounds robustly reduced Cl^- efflux in isolated pancreatic ductal fragments, supporting that CFTR activity in this context is strongly dependent on PKA-mediated phosphorylation (**Figure 25/B.**). These observations suggest that the Ca^{2+}-stimulated AC1/3/8 act via PKA in a signalling nanodomain with a dominant role of the lipid raft-associated AC8 to translate the stimulatory effect of SICE via ORAI1 on cAMP elevation and increased basal CFTR activity.

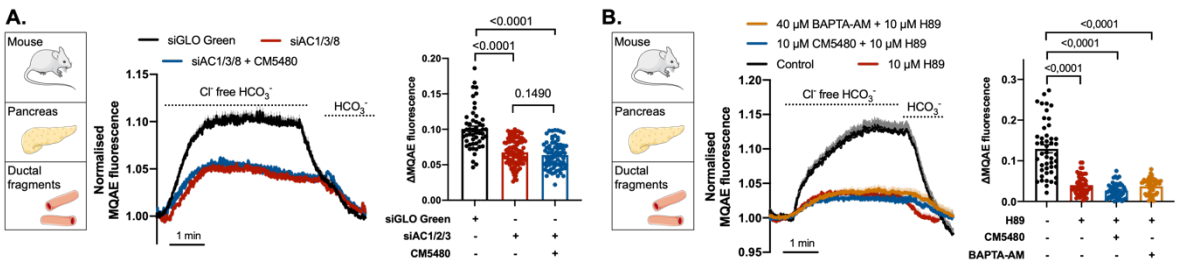

Figure 25. A. Average traces and summary bar charts from 4 to 6 independent experiments show that individual gene silencing of AC1, AC3, or AC8 significantly reduced CFTR-mediated anion secretion, assessed by MQAE fluorescence upon Cl^- withdrawal, in apical-out human pancreatic organoids. **B.** Average traces and corresponding bar charts show that treatment with 100 nM PKI (5–24) (red) or 1 μM KT5720 (blue) significantly reduced Cl^- efflux, compared with vehicle-treated controls (black), upon Cl^-/HCO_3^- exchange. Data are presented as mean ± SEM.

9. DISCUSSION

CFTR Cl^- channel fundamentally determines transepithelial ion and fluid secretion and hence hydration of different organs' luminal surfaces; moreover, basal CFTR activity is required to maintain hydration of the luminal surfaces even when stimulated secretion is not activated. Therefore, proper spatiotemporal regulation of the channel activity is essential for life. This study identified and comprehensively characterized a novel regulatory mechanism determining basal CFTR activity in unstimulated primary polarized epithelial cells independently of neurohormonal stimuli. By applying state-of-the-art molecular biology and imaging techniques, we describe a highly organized signalling nanodomain on the apical PM of epithelial cells from mouse and human tissues, including the pancreas, liver, and lung. In this nanodomain, SPCA2 maintains constitutive interaction between STIM1/ORAI1 in a Ca^{2+} store-independent manner, leading to a constitutive extracellular Ca^{2+} influx. The SICE initiated by SPCA2 maintains the activity of the Ca^{2+}-dependent ACs that determine basal CFTR activity and fluid secretion in secretory epithelial cells.

The molecular components of SOCE, STIM1, and ORAI1 are ubiquitously expressed (37,75). In this study, we showed that ORAI1 is primarily expressed on the apical membrane of polarized secretory epithelial cells in the pancreas, liver, and airway. Surprisingly, we found that ORAI1-mediated Ca^{2+} influx is constitutively active, significantly contributing to basal Ca^{2+} levels in these cells. This constitutive activity was absent in pancreatic acinar cells, where ORAI1 activates only after store depletion (72,76). While previous studies mainly focused on the pathological roles of ORAI1 (77), the physiological functions and mechanisms of ORAI1-mediated SICE remain poorly understood. Previously, Feng et al. demonstrated that the ORAI1-SPCA2 complex elicits constitutive store- and STIM1-independent Ca^{2+} signalling that promotes tumorigenesis in breast cancer-derived cells (48). Here, we show that the constitutive ORAI1 activity in polarized epithelial cells is independent of ER Ca^{2+} store depletion; however, it requires STIM1 and is activated by SPCA2. Previously, the overexpression of SPCA1 was also reported to induce cytosolic Ca^{2+} influx (45). However, our knockdown experiments suggested that in primary epithelial cells, the regulation is specific to SPCA2 and is not affected by SPCA1. Unlike ubiquitously expressed SPCA1 (78), SPCA2 expression is tissue specific (79), possibly explaining why SICE occurs in secretory epithelia but not in acinar cells. In the pancreatic acinar cells, previous studies identified a specific isoform of SPCA2 (termed SPCA2C) (80), which was involved in the regulation of Ca^{2+} homeostasis, when expressed in HEK293 cells (81). In contrast, secretory epithelial cells, including pancreatic ductal cells,

express the full-length SPCA2 (82). In addition, previous studies suggest that both the N′ - and C′-terminal domains of SPCA2 have important functions in the protein-protein interactions (50).

In our experiments, SPCA2 displayed a reticular expression pattern enriched at the apical pole of polarized epithelial cells. Mechanistically, SPCA2 enhanced unstimulated puncta formation of ORAI1 and the STIM1-ORAI1 complex independently of ER Ca^{2+} depletion. However, SPCA2 did not increase basal STIM1 puncta formation without exogenous ORAI1 overexpression, suggesting that SPCA2 primarily targets ORAI1. The clustered ORAI1 can recruit and stabilize STIM1 in the puncta, as it is known that ORAI1 reduces STIM1 mobility to stabilize STIM1 clustering (83). Notably, the activation of ORAI1 by SPCA2 did not reach the level of maximal ORAI1 activation. The FLIM- FRET measurements also revealed that SPCA2 and ORAI1 are in physical proximity in unstimulated cells, which is in line with the previous findings (48). Of note, the ER Ca^{2+} depletion decreased co-cluster area of SPCA2 and ORAI1; however, the FRET efficiency was not increased further, which could be explained by the redistribution of the ER in response to Ca^{2+} depletion (84).

CFTR-mediated ion secretion is a critical rate-limiting step in secretory epithelial cells; thus, we examined how SPCA2-triggered SICE affects CFTR activity. Previous studies suggest that the co-localization of these proteins as mutations in CFTR affected ORAI1 channel function and enhanced ORAI1-mediated Ca^{2+} influx, leading to increased interleukin-8 (IL-8) secretion in airway cells (85). Even more importantly, Shan et al. described that CFTR has basal activity that was inhibited by the administration of 2-APB (2-Aminoethyl diphenyl borinate), a non-selective inhibitor of ORAI1 (86). The authors also showed that the basal current was also markedly reduced by MDL-12330A, a membrane-bound AC antagonist, and by the PKA inhibitor Rp-cAMPS (Rp-Adenosine-3',5'-cyclic monophosphorothioate). These findings indicate that basal CFTR activity depends on local cAMP production by membrane-bound ACs activated by Ca^{2+} influx through ORAI1 channels. Moreover, a recent study showed that the nasal epithelium displays constitutive CFTR activity, which is essential to maintain viscoelastic properties of the mucus layer and to mucociliary transport (87). Here, we directly showed that CFTR and ORAI1 closely co- localize (~20–30 nm apart) on the apical membrane of pancreatic, liver, and airway epithelial cells, providing the first direct evidence for their assembly into a signalling complex nanodomain. Functional assays revealed that both pharmacologic inhibition or gene silencing of STIM1 and ORAI1 impaired CFTR activity and abolished unstimulated basal fluid secretion. In contrast, forskolin-induced CFTR activity

remained intact when ORAI1 was inhibited, indicating that SICE regulates basal but not stimulated CFTR activity.

Previously, we and others showed that sustained, uncontrolled ORAI1 activation increases intracellular Ca^{2+} levels, causing cell damage in various diseases (72,88,89). However, our results indicate that constitutive ORAI1 activity is necessary to maintain resting Ca^{2+} levels and basal CFTR activity in secretory epithelial cells. Notably, the Ca^{2+} changes due to SPCA2/ORAI1 interactions are smaller than those from stimulated responses, possibly due to limitations of the cytoplasmic dye (FURA2-AM), which average signals across the entire cell and are not accumulated at or targeted to a specific subcellular region. Large, prolonged Ca^{2+} elevations can be toxic, often leading to ER stress and cell death (90). Thus, continuous SICE likely induces localized Ca^{2+} nanodomains near the CFTR-expressing subplasmalemmal regions, rather than widespread increases, supporting physiological functions without the depletion of ER stores and ER stress. Our findings also raise the possibility that distinct ORAI1 pools exist in specific PM nanodomains of polarized cells, regulating channel function and store-dependent or -independent activities.

Finally, we wanted to provide mechanistic insight into how SPCA2/STIM1/ORAI1-mediated SICE determines CFTR activity. Independent studies suggest synergism between cAMP and Ca^{2+} signalling that is crucial in regulating secretory epithelial cells' physiological functions (23). One form of synergism is the divergent regulation of AC protein activities by Ca^{2+}, which can affect CFTR activity (91). Another example is the action of IP3R-binding protein released with InsP3 (IRBIT) in pancreatic ductal epithelia (92), which significantly improved the dose response of CFTR to forskolin or carbachol, independently of cytoplasmic Ca^{2+}. Our experiments revealed that SICE in epithelial cells controls CFTR activity in a PKA-dependent manner, which suggests that the enhanced cAMP synthesis by ACs is a critical step in the process. Whole-transcriptome analysis of mouse and human pancreatic ductal organoids revealed the expression of AC1, 3, 5, 6, 7, 8, and 9 in the ductal epithelia, and the highest expression was observed in the case of AC6. Sabbatini et al. previously showed that AC6 knockout mice had reduced cAMP generation, PKA activation, and impaired fluid secretion after hormonal stimulation (93). However, AC6 is inhibited by Ca^{2+} and thus unlikely to mediate SICE. Earlier studies indicated direct interactions between the amino termini AC8 and ORAI1 coordinating Ca^{2+} and cAMP signalling (94), while STIM1 translocation upon ER Ca^{2+} depletion enhanced AC-mediated cAMP independently of cytosolic Ca^{2+} levels (95). Previous studies in bronchial epithelial cells report that compartmentalized AC1-CFTR interaction is responsible for Ca^{2+}/cAMP cross-talk in response to purinergic stimulation that also influence

the activity of TMEM16A (35,96). Our dSTORM analysis showed that CFTR closely co-localizes with AC1, AC3, and AC8—but only moderately with AC6—in PM nanodomains containing ORAI1. Knockdown of AC1/3/8 reduced basal CFTR activity, and the most significant decrease was achieved by siAC8 treatment. We also showed that the deletion of the N-terminal domain of ORAI1 markedly reduced co-localization with AC8, whereas the AC8 had significantly higher activity in the lipid rafts. Our results also suggest that the inhibition of ORAI1 decreases CFTR activity via the impaired generation of the local cAMP pool and PKA activity. These results are in line with previous observations (94,97,98) and also highlight that CFTR is at least partially associated with lipid raft domains of the PM. A previous study identified two populations of CFTR at the cell surface distinguished based on their dynamics that were highly cholesterol dependent in the first group, providing biophysical evidence for multiple CFTR populations in the PM (99). This observation and our finding also raise the possibility that different CFTR subpopulations play a role in basal and stimulated secretion. Moreover, our recent study revealed that epithelial secretion depends on phosphatidylserine (PtdSer) levels in the ER/PM junctions, regulated by opposing actions of lipid transfer proteins E-Syt3 and ORP5 (100). Altering junctional PtdSer by E-Syt3 disrupted CFTR and NBCe1-B activation, while E-Syt3 depletion enhanced Cl^- flux and fluid secretion in mouse epithelial tissues.

Three-dimensional organoid cultures derived from human pancreatic ductal tissue provide a highly physiologically relevant system to study epithelial structure and function. These organoids consist of a single layer of polarized epithelial cells enclosing a central lumen, closely resembling the organization of native pancreatic ducts. Under culture conditions supporting Wnt/β-catenin signalling (64,65), the cells maintain their ductal identity, junctional integrity, and apical–basal polarity, which together enable the investigation of epithelial processes such as ion secretion, fluid transport, and intracellular signalling in a near-physiological setting.

Compared to traditional immortalized cell lines, pancreatic organoids offer several distinct advantages. Conventional monolayer cultures often lose polarity, show altered gene expression, and fail to reproduce the coordinated ion transport that characterizes ductal epithelia *in vivo*. In contrast, organoid cultures preserve tight junctions and maintain vectorial secretion, resulting in measurable luminal fluid accumulation. This allows the application of functional assays, such as forskolin-induced swelling or live-cell Ca^{2+} imaging, to directly assess ductal ion channel activity under controlled conditions (52,58,59,66). Furthermore, organoids derived from human tissue retain donor-specific genetic and physiological traits, making them highly suitable for

translational studies and disease modelling, including CF and inflammatory pancreatic disorders (53,57,58).

In our study, we used conventional human pancreatic organoids to investigate the mechanisms that determine basal CFTR activity and its dependence on Ca^{2+} signalling. This model provided a unique opportunity to analyse how intracellular Ca^{2+} dynamics contribute to the regulation of CFTR-mediated ion and fluid secretion in a structurally intact epithelial context. We specifically focused on the role of the store-independent Ca^{2+} entry pathway governed by the SPCA2–STIM1–ORAI1 complex. Previous studies had identified this signalling axis as a key determinant of resting Ca^{2+} levels in secretory epithelial cells; however, its functional link to CFTR had not been characterized in human ductal tissue. Using the organoid model, we demonstrated that SPCA2-driven activation of STIM1 and ORAI1 sustains a low-level, constitutive Ca^{2+} influx that supports basal CFTR activity even in the absence of external stimulation.

The organoid approach was essential for these experiments, as it allowed us to assess Ca^{2+} handling and CFTR function in cells maintaining their native polarity and intercellular organization—conditions that cannot be replicated in two-dimensional cultures. The preserved epithelial architecture enabled accurate measurement of vectorial secretion and the analysis of apical and basolateral signalling domains within the same structure. Moreover, the three-dimensional system provides a stable baseline for pharmacological or genetic manipulation, making it suitable for dissecting how specific molecular pathways, such as store-independent Ca^{2+} entry, integrate into the regulation of epithelial transport processes.

The human pancreatic organoid model represents an advanced experimental platform that bridges the gap between conventional cell lines and *in vivo* systems. Its physiological relevance, structural integrity, and functional stability make it ideally suited for exploring the molecular mechanisms underlying Ca^{2+}-dependent regulation of CFTR and other secretory processes in the pancreatic ductal epithelium.

In summary, we describe a novel mechanism in which SPCA2 regulates epithelial ion secretion through STIM1/ORAI1-mediated constitutive Ca^{2+} influx, essential for basal CFTR activity in polarized secretory epithelial cells. Moreover, we identified a protein nanodomain on the apical membrane composed of SPCA2/STIM1/ORAI1, CFTR, and Ca^{2+}-activated AC1, 3, and 8, highlighting distinct regulatory mechanisms for basal versus stimulated secretion. Our model proposes that constitutive Ca^{2+} influx maintains basal CFTR activity independently of neurohormonal stimulation that adjust the ion and fluid secretion to various stimuli. Importantly, this nanodomain may also impact cancer biology, as SPCA2 promotes breast

cancer progression (101), loss of CFTR expression is linked to enhanced Wnt/β-catenin signalling and tumor risk in CF (102), and ORAI1 regulates proliferation and metastasis (103). Understanding ORAI1/SPCA2 interactions may therefore uncover novel therapeutic targets for cancer.

10. SUMMARY

The CFTR Cl^- channel is essential for maintaining transepithelial ion and fluid secretion, ensuring proper hydration of epithelial surfaces such as those in the pancreas, liver, and lungs. While CFTR activation during stimulated secretion is well studied, the mechanisms underlying its basal activity—which sustains luminal hydration in the absence of external stimuli—remain poorly understood. This study identifies a novel regulatory mechanism responsible for maintaining basal CFTR function through a store-independent Ca^{2+} entry (SICE) pathway mediated by the SPCA2/STIM1/ORAI1 complex in polarized epithelial cells.

Using advanced molecular and imaging techniques in both mouse and human tissues, we described a highly organized signalling nanodomain localized to the apical plasma membrane of secretory epithelial cells. Within this nanodomain, SPCA2 (Secretory Pathway Ca^{2+}-ATPase 2) interacts with STIM1 and ORAI1 to sustain constitutive Ca^{2+} influx independent of endoplasmic reticulum (ER) Ca^{2+} store depletion. This influx maintains the activity of Ca^{2+}-dependent ACs, which in turn produce cyclic AMP (cAMP) necessary for basal PKA-dependent CFTR activation.

Unlike SPCA1, which is ubiquitously expressed, SPCA2 shows tissue-specific expression, explaining its presence in secretory epithelia but absence in pancreatic acinar cells. SPCA2 promotes clustering of ORAI1 and stabilizes STIM1–ORAI1 complexes even without ER Ca^{2+} depletion, enhancing basal Ca^{2+} entry. Electrophysiological and FRET analyses confirmed that SPCA2 and ORAI1 are in close physical proximity and that SPCA2 can activate ORAI1 channels independently of its ATPase activity.

Functional studies revealed that constitutive ORAI1 activity is essential for maintaining basal intracellular Ca^{2+} levels and CFTR function. Pharmacological inhibition or gene silencing of SPCA2, STIM1, or ORAI1 reduced basal CFTR-mediated Cl^- currents and fluid secretion, while forskolin-induced (stimulated) CFTR activity remained unaffected. These findings indicate that SICE specifically controls basal, but not hormone-stimulated, CFTR activity.

High-resolution dSTORM microscopy revealed that CFTR, ORAI1, SPCA2, STIM1, and Ca^{2+}-activated AC1, AC3, and AC8 co-localize within 20–30 nm nanodomains on the apical membrane. Silencing these AC isoforms, especially AC8, markedly reduced basal CFTR activity, confirming their role in local cAMP generation. The spatial proximity of ORAI1 and AC8 suggests that Ca^{2+} influx through ORAI1 directly activates AC8 to generate localized cAMP pools that stimulate PKA and CFTR. This mechanism establishes a Ca^{2+}/cAMP crosstalk

critical for basal secretion. Furthermore, lipid raft localization of these complexes implies the existence of distinct CFTR subpopulations responsible for basal versus stimulated secretion.

The study proposes that SPCA2-activated SICE forms a self-sustaining signalling microdomain that integrates Ca^{2+} influx, cAMP synthesis, and CFTR activation, ensuring basal hydration of epithelial surfaces. This mechanism operates independently of neurohormonal input and provides a fine-tuned regulatory system to maintain epithelial homeostasis **(Figure 26.)**.

Beyond physiology, these findings may have pathological relevance. Dysregulation of SPCA2 or ORAI1 is implicated in cancer progression, while CFTR loss is linked to enhanced Wnt/β-catenin signalling and increased tumor risk in CF. Thus, understanding the molecular architecture and regulation of the SPCA2/STIM1/ORAI1 nanodomain could uncover new therapeutic targets for diseases involving epithelial dysfunction or malignancy.

In conclusion, our study uncovers a previously unrecognized, store-independent Ca^{2+} entry mechanism that sustains basal CFTR activity in secretory epithelial cells. The discovery of the SPCA2/STIM1/ORAI1/AC/CFTR nanodomain provides new insights into how epithelial tissues maintain fluid secretion under resting conditions and highlights the intricate spatial organization of ion signalling networks that underpin essential physiological and pathological processes.

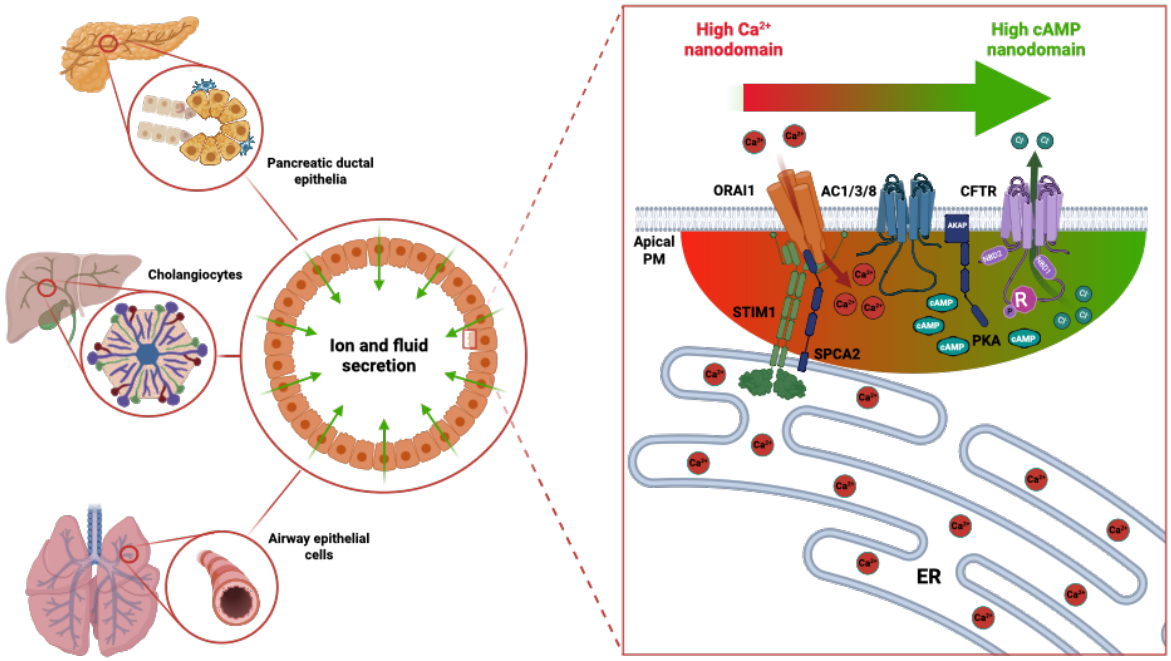

Figure 26. Summary figure of the signalling network between the Ca^{2+} and cAMP nanodomain in liver, lung and pancreatic epithelial cells.

11. SUMMARY OF NEW OBSERVATIONS

1. We revealed that in polarized secretory epithelial cells, CFTR activity is maintained under resting conditions by a constitutive, store-independent Ca^{2+} influx rather than by classical neurohormonal stimuli.
2. SPCA2 was identified as a central regulator that activates the STIM1–ORAI1 complex in the absence of ER Ca^{2+} depletion. This SPCA2-dependent SICE provides a continuous Ca^{2+} source required for maintaining basal epithelial ion and fluid secretion.
3. Pharmacological or genetic inhibition of STIM1 or ORAI1 reduced basal CFTR activity and resting fluid secretion, while stimulated (forskolin-induced) responses remained intact.
4. The results support a model in which SPCA2 continuously activates ORAI1-mediated Ca^{2+} influx that, via Ca^{2+}-activated ACs, generates local cAMP and PKA activity sustaining basal CFTR function. This mechanism operates independently of ER Ca^{2+} depletion or neurohormonal stimulation and defines a distinct regulatory layer of epithelial homeostasis.

12. ACKNOWLEDGEMENTS

Scientific work is never a solitary endeavour, and I have been incredibly fortunate to be surrounded by mentors, colleagues, friends, and family who have guided, inspired, and supported me throughout this journey. First and foremost, I want to express my deepest gratitude to my supervisor, **József Maléth**. His guidance, insight, and encouragement have been invaluable throughout my doctoral studies. His support not only shaped this thesis but also made the challenges of research truly rewarding.

I am grateful to **Prof. Dr. Csaba Lengyel**, the current head of the Department of Internal Medicine, who gave me the opportunity to work in his department.

I am especially grateful to **Árpád Varga**, who had been my mentor for seven years. From my BSc studies his guidance has been a constant source of learning. I have gained an immense amount from his expertise, patience, and the countless lessons he has shared. Beyond his invaluable scientific guidance, I am deeply thankful for his friendship, which has made these years even more meaningful.

I would like to express my deepest appreciation to those with whom we have accompanied each other on this journey, **Tamara Madácsy, Zsófia Horváth, Tünde Molnár, Viktória Szabó, Boldizsár Jójárt, Petra Susánszki, Noémi Papp**. I'm grateful for all your help, encouragement, and the great times we had together, without their inspiration, this project would not have been possible. I am deeply grateful to all my colleagues who have taught, helped and supported me over the years, **Petra Pallagi, Enikő Kúthy-Sutus, Tim Crul, Bálint Tél, Ingrid Hegnes Sendstad, Marietta Görög, Krisztina Dudás, Melinda Molnár, Zsuzsanna Sáriné Konczos, Anita Zsirmik, Edit Magyarné Pálfi, Gabriella Fűr.**

To my friends, who have stood by me through long days in the lab and busy periods of writing, I am profoundly grateful. Your patience, support, and belief in me made this journey much more meaningful. Finally, I owe my deepest thanks to my family. I am especially grateful to my grandmother **Etelka Kukityné Gyapjas**, whose unwavering love, support, and sacrifices have made this achievement possible—without her, I would not have reached this point. I also want to acknowledge my mother **Katalin Kukity** for her constant encouragement and belief in me. I hope that my late father **Tibor Botka** would be proud of me and of all that I have accomplished. Their guidance and the values they instilled in me have been a constant source of strength throughout my life.

13. REFERENCES

1. Khan S, Fitch S, Knox S, Arora R. Exocrine gland structure-function relationships. Development. 2022 Jan 1;149(1):dev197657.

2. Frizzell RA, Hanrahan JW. Physiology of Epithelial Chloride and Fluid Secretion. Cold Spring Harbor Perspectives in Medicine. 2012 June 1;2(6):a009563–a009563.

3. Park HW, Lee MG. Transepithelial Bicarbonate Secretion: Lessons from the Pancreas. Cold Spring Harbor Perspectives in Medicine. 2012 Oct 1;2(10):a009571–a009571.

4. Ishiguro H, Yamamoto A, Nakakuki M, Yi L, Ishiguro M, Yamaguchi M, et al. physiology and Pathophysiology of bicarbonate secretion by pancreatic duct epithelium.

5. Button BM, Button B. Structure and Function of the Mucus Clearance System of the Lung. Cold Spring Harbor Perspectives in Medicine. 2013 Aug 1;3(8):a009720–a009720.

6. Figueira MF, Ribeiro CMP, Button B. Mucus-targeting therapies of defective mucus clearance for cystic fibrosis: A short review. Current Opinion in Pharmacology. 2022 Aug;65:102248.

7. Saint-Criq V, Gray MA. Role of CFTR in epithelial physiology. Cell Mol Life Sci. 2017 Jan;74(1):93–115.

8. Slippery When Wet. In: Current Topics in Membranes [Internet]. Elsevier; 2018 [cited 2025 Oct 21]. p. 293–335. Available from: https://linkinghub.elsevier.com/retrieve/pii/S1063582318300127

9. Lee MG, Ohana E, Park HW, Yang D, Muallem S. Molecular Mechanism of Pancreatic and Salivary Gland Fluid and HCO_3^- Secretion. Physiological Reviews. 2012 Jan;92(1):39–74.

10. Hanssens LS, Duchateau J, Casimir GJ. CFTR Protein: Not Just a Chloride Channel? Cells. 2021 Oct 22;10(11):2844.

11. Tümmler B. Puzzle resolved: CFTR mediates chloride homeostasis by segregating absorption and secretion to different cell types. Journal of Clinical Investigation. 2023 Oct 16;133(20):e174667.

12. Borowitz D. CFTR, bicarbonate, and the pathophysiology of cystic fibrosis. Pediatric Pulmonology [Internet]. 2015 Oct [cited 2025 Oct 22];50(S40). Available from: https://onlinelibrary.wiley.com/doi/10.1002/ppul.23247

13. Mall MA, Burgel PR, Castellani C, Davies JC, Salathe M, Taylor-Cousar JL. Cystic fibrosis. Nat Rev Dis Primers. 2024 Aug 8;10(1):53.

14. Ramananda Y, Naren AP, Arora K. Functional Consequences of CFTR Interactions in Cystic Fibrosis. IJMS. 2024 Mar 16;25(6):3384.

15. Mihályi C, Töröcsik B, Csanády L. Obligate coupling of CFTR pore opening to tight nucleotide-binding domain dimerization. eLife. 2016 June 21;5:e18164.

16. Wu M, Xiong Y, Cao M, Zhi Y, Jin Y, Huang Y, et al. A cluster of inhibitory residues in the regulatory domain prevents activation of the cystic fibrosis transmembrane conductance regulator. Journal of Biological Chemistry. 2025 May;301(5):108460.

17. Della Sala A, Prono G, Hirsch E, Ghigo A. Role of Protein Kinase A-Mediated Phosphorylation in CFTR Channel Activity Regulation. Front Physiol. 2021 June 11;12:690247.

18. Murabito A, Bhatt J, Ghigo A. It Takes Two to Tango! Protein–Protein Interactions behind cAMP-Mediated CFTR Regulation. IJMS. 2023 June 23;24(13):10538.

19. Li C. Compartmentalized Regulation of CFTR Chloride Channel Function in Apical Epithelia. J Proteomics Bioinform [Internet]. 2013 [cited 2025 Oct 22];06(10). Available from: https://www.omicsonline.org/compartmentalized-regulation-of-cftr-chloride-channel-function-in-apical-epithelia-jpb.1000283.php?aid=2549

20. Bozoky Z, Krzeminski M, Chong PA, Forman-Kay JD. Structural changes of CFTR R region upon phosphorylation: a plastic platform for intramolecular and intermolecular interactions. The FEBS Journal. 2013 Sept;280(18):4407–16.

21. Mihályi C, Iordanov I, Töröcsik B, Csanády L. Simple binding of protein kinase A prior to phosphorylation allows CFTR anion channels to be opened by nucleotides. Proc Natl Acad Sci USA. 2020 Sept;117(35):21740–6.

22. Sun F, Hug MJ, Bradbury NA, Frizzell RA. Protein Kinase A Associates with Cystic Fibrosis Transmembrane Conductance Regulator via an Interaction with Ezrin. Journal of Biological Chemistry. 2000 May;275(19):14360–6.

23. Ahuja M, Jha A, Maléth J, Park S, Muallem S. cAMP and Ca2+ signaling in secretory epithelia: Crosstalk and synergism. Cell Calcium. 2014 June;55(6):385–93.

24. Ahuja M, Chung WY, Lin WY, McNally BA, Muallem S. Ca^{2+} Signaling in Exocrine Cells. Cold Spring Harb Perspect Biol. 2020 May;12(5):a035279.

25. Fiedorczuk K, Iordanov I, Mihályi C, Szollosi A, Csanády L, Chen J. The structures of protein kinase A in complex with CFTR: Mechanisms of phosphorylation and noncatalytic activation. Proc Natl Acad Sci USA. 2024 Nov 12;121(46):e2409049121.

26. Chen JH. Protein kinase A phosphorylation potentiates cystic fibrosis transmembrane conductance regulator gating by relieving autoinhibition on the

stimulatory C terminus of the regulatory domain. Journal of Biological Chemistry. 2020 Apr;295(14):4577–90.

27. Li J, Dai Z, Jana D, Callaway DJE, Bu Z. Ezrin Controls the Macromolecular Complexes Formed between an Adapter Protein Na+/H+ Exchanger Regulatory Factor and the Cystic Fibrosis Transmembrane Conductance Regulator. Journal of Biological Chemistry. 2005 Nov;280(45):37634–43.

28. Blanchard E, Zlock L, Lao A, Mika D, Namkung W, Xie M, et al. Anchored PDE4 regulates chloride conductance in wild-type and ΔF508-CFTR human airway epithelia. FASEB j. 2014 Feb;28(2):791–801.

29. Baillie GS, Tejeda GS, Kelly MP. Therapeutic targeting of 3',5'-cyclic nucleotide phosphodiesterases: inhibition and beyond. Nat Rev Drug Discov. 2019 Oct;18(10):770–96.

30. Madácsy T, Pallagi P, Maleth J. Cystic Fibrosis of the Pancreas: The Role of CFTR Channel in the Regulation of Intracellular Ca2+ Signaling and Mitochondrial Function in the Exocrine Pancreas. Front Physiol. 2018 Dec 20;9:1585.

31. Kunzelmann K, Mehta A. CFTR : a hub for kinases and crosstalk of c AMP and C a^{2+}. The FEBS Journal. 2013 Sept;280(18):4417–29.

32. Bozoky Z, Ahmadi S, Milman T, Kim TH, Du K, Di Paola M, et al. Synergy of cAMP and calcium signaling pathways in CFTR regulation. Proc Natl Acad Sci USA. 2017 Mar 14;114(11):E2086–95.

33. Billet A, Hanrahan JW. The secret life of CFTR as a calcium-activated chloride channel. The Journal of Physiology. 2013 Nov;591(21):5273–8.

34. Willoughby D, Cooper DMF. Organization and Ca^{2+}Regulation of Adenylyl Cyclases in cAMP Microdomains. Physiological Reviews. 2007 July;87(3):965–1010.

35. Namkung W, Finkbeiner WE, Verkman AS. CFTR-Adenylyl Cyclase I Association Responsible for UTP Activation of CFTR in Well-Differentiated Primary Human Bronchial Cell Cultures. Margolis B, editor. MBoC. 2010 Aug;21(15):2639–48.

36. Concepcion AR, Vaeth M, Wagner LE, Eckstein M, Hecht L, Yang J, et al. Store-operated Ca2+ entry regulates Ca2+-activated chloride channels and eccrine sweat gland function. Journal of Clinical Investigation. 2016 Oct 10;126(11):4303–18.

37. Prakriya M, Lewis RS. Store-Operated Calcium Channels. Physiol Rev. 2015;95.

38. Liou J, Kim ML, Do Heo W, Jones JT, Myers JW, Ferrell JE, et al. STIM Is a Ca2+ Sensor Essential for Ca2+-Store-Depletion-Triggered Ca2+ Influx. Current Biology. 2005 July;15(13):1235–41.

39. Park CY, Hoover PJ, Mullins FM, Bachhawat P, Covington ED, Raunser S, et al. STIM1 Clusters and Activates CRAC Channels via Direct Binding of a Cytosolic Domain to Orai1. Cell. 2009 Mar;136(5):876–90.

40. Liou J, Kim ML, Do Heo W, Jones JT, Myers JW, Ferrell JE, et al. STIM Is a Ca2+ Sensor Essential for Ca2+-Store-Depletion-Triggered Ca2+ Influx. Current Biology. 2005 July;15(13):1235–41.

41. Jairaman A, Prakriya M. Calcium Signaling in Airway Epithelial Cells: Current Understanding and Implications for Inflammatory Airway Disease. ATVB. 2024 Apr;44(4):772–83.

42. Prakriya M, Feske S, Gwack Y, Srikanth S, Rao A, Hogan PG. Orai1 is an essential pore subunit of the CRAC channel. Nature. 2006 Sept;443(7108):230–3.

43. Zhang X, Zhang W, González-Cobos JC, Jardin I, Romanin C, Matrougui K, et al. Complex role of STIM1 in the activation of store-independent Orai1/3 channels. Journal of General Physiology. 2014 Mar 1;143(3):345–59.

44. Schober R, Waldherr L, Schmidt T, Graziani A, Stilianu C, Legat L, et al. STIM1 and Orai1 regulate Ca2+ microdomains for activation of transcription. Biochimica et Biophysica Acta (BBA) - Molecular Cell Research. 2019 July;1866(7):1079–91.

45. Smaardijk S, Chen J, Kerselaers S, Voets T, Eggermont J, Vangheluwe P. Store-independent coupling between the Secretory Pathway Ca2+ transport ATPase SPCA1 and Orai1 in Golgi stress and Hailey-Hailey disease. Biochimica et Biophysica Acta (BBA) - Molecular Cell Research. 2018 June;1865(6):855–62.

46. Makena MR, Ko M, Mekile AX, Senoo N, Dang DK, Warrington J, et al. Secretory pathway Ca2+-ATPase SPCA2 regulates mitochondrial respiration and DNA damage response through store-independent calcium entry. Redox Biology. 2022 Apr;50:102240.

47. Chen J, Smaardijk S, Mattelaer CA, Pamula F, Vandecaetsbeek I, Vanoevelen J, et al. An N-terminal Ca2+-binding motif regulates the secretory pathway Ca2+/Mn2+-transport ATPase SPCA1. Journal of Biological Chemistry. 2019 May;294(19):7878–91.

48. Feng M, Grice DM, Faddy HM, Nguyen N, Leitch S, Wang Y, et al. Store-Independent Activation of Orai1 by SPCA2 in Mammary Tumors. Cell. 2010 Oct;143(1):84–98.

49. Cross BM, Hack A, Reinhardt TA, Rao R. SPCA2 Regulates Orai1 Trafficking and Store Independent Ca2+ Entry in a Model of Lactation. Obukhov AG, editor. PLoS ONE. 2013 June 28;8(6):e67348.

50. Girault A, Peretti M, Badaoui M, Hémon A, Morjani H, Ouadid-Ahidouch H. The N and C-termini of SPCA2 regulate differently Kv10.1 function: role in the collagen 1-induced breast cancer cell survival.

51. Smaardijk S, Chen J, Wuytack F, Vangheluwe P. SPCA2 couples Ca 2+ influx via Orai1 to Ca 2+ uptake into the Golgi/secretory pathway. Tissue and Cell. 2017 Apr;49(2):141–9.

52. Boj SF, Hwang CI, Baker LA, Chio IIC, Engle DD, Corbo V, et al. Organoid Models of Human and Mouse Ductal Pancreatic Cancer. Cell. 2015 Jan;160(1–2):324–38.

53. Baker L, Tiriac H, Corbo V, Young CM. Tuveson Laboratory Murine and Human Organoid Protocols.

54. Barker N, van Es JH, Kuipers J, Kujala P, van den Born M, Cozijnsen M, et al. Identification of stem cells in small intestine and colon by marker gene Lgr5. Nature. 2007 Oct;449(7165):1003–7.

55. Haegebarth A, Clevers H. Wnt Signaling, Lgr5, and Stem Cells in the Intestine and Skin. The American Journal of Pathology. 2009 Mar;174(3):715–21.

56. Sato T, Vries RG, Snippert HJ, Van De Wetering M, Barker N, Stange DE, et al. Single Lgr5 stem cells build crypt-villus structures in vitro without a mesenchymal niche. Nature. 2009 May;459(7244):262–5.

57. Casamitjana J, Espinet E, Rovira M. Pancreatic Organoids for Regenerative Medicine and Cancer Research. Front Cell Dev Biol. 2022 May 3;10:886153.

58. Clevers H. Modeling Development and Disease with Organoids. Cell. 2016 June;165(7):1586–97.

59. Molnár R, Madácsy T, Varga Á, Németh M, Katona X, Görög M, et al. Mouse pancreatic ductal organoid culture as a relevant model to study exocrine pancreatic ion secretion. Lab Invest. 2020 Jan;100(1):84–97.

60. Miller AJ, Dye BR, Ferrer-Torres D, Hill DR, Overeem AW, Shea LD, et al. Generation of lung organoids from human pluripotent stem cells in vitro. Nat Protoc. 2019 Feb;14(2):518–40.

61. Garnier D, Li R, Delbos F, Fourrier A, Collet C, Guguen-Guillouzo C, et al. Expansion of human primary hepatocytes in vitro through their amplification as liver progenitors in a 3D organoid system. Sci Rep. 2018 May 29;8(1):8222.

62. Wallach TE, Bayrer JR. Intestinal Organoids: New Frontiers in the Study of Intestinal Disease and Physiology. J pediatr gastroenterol nutr. 2017 Feb;64(2):180–5.

63. Moreira L, Bakir B, Chatterji P, Dantes Z, Reichert M, Rustgi AK. Pancreas 3D Organoids: Current and Future Aspects as a Research Platform for Personalized Medicine in Pancreatic Cancer. Cellular and Molecular Gastroenterology and Hepatology. 2018;5(3):289–98.

64. Carmon KS, Gong X, Lin Q, Thomas A, Liu Q. R-spondins function as ligands of the orphan receptors LGR4 and LGR5 to regulate Wnt/β-catenin signaling. Proc Natl Acad Sci USA. 2011 July 12;108(28):11452–7.

65. Nusse R, Clevers H. Wnt/β-Catenin Signaling, Disease, and Emerging Therapeutic Modalities. Cell. 2017 June;169(6):985–99.

66. Varga Á, Madácsy T, Görög M, Kiss A, Susánszki P, Szabó V, et al. Human pancreatic ductal organoids with controlled polarity provide a novel ex vivo tool to study epithelial cell physiology. Cell Mol Life Sci. 2023 July;80(7):192.

67. Argent BE, Arkle S, Cullen MJ, Green R. MORPHOLOGICAL, BIOCHEMICAL AND SECRETORY STUDIES ON RAT PANCREATIC DUCTS MAINTAINED IN TISSUE CULTURE. Exp Physiol. 1986 Oct 10;71(4):633–48.

68. Maléth J, Balázs A, Pallagi P, Balla Z, Kui B, Katona M, et al. Alcohol Disrupts Levels and Function of the Cystic Fibrosis Transmembrane Conductance Regulator to Promote Development of Pancreatitis. Gastroenterology. 2015 Feb;148(2):427-439.e16.

69. Fanczal J, Pallagi P, Görög M, Diszházi G, Almássy J, Madácsy T, et al. TRPM2-mediated extracellular Ca^{2+} entry promotes acinar cell necrosis in biliary acute pancreatitis. The Journal of Physiology. 2020 Mar;598(6):1253–70.

70. Venglovecz V, Hegyi P, Rakonczay Z, Tiszlavicz L, Nardi A, Grunnet M, et al. Pathophysiological relevance of apical large-conductance Ca2+-activated potassium channels in pancreatic duct epithelial cells. Gut. 2011 Mar 1;60(3):361–9.

71. Pallagi P, Balla Z, Singh AK, Dósa S, Iványi B, Kukor Z, et al. The Role of Pancreatic Ductal Secretion in Protection Against Acute Pancreatitis in Mice*: Critical Care Medicine. 2014 Mar;42(3):e177–88.

72. Szabó V, Csákány-Papp N, Görög M, Madácsy T, Varga Á, Kiss A, et al. Orai1 calcium channel inhibition prevents progression of chronic pancreatitis.

73. Wu MM, Buchanan J, Luik RM, Lewis RS. Ca2+ store depletion causes STIM1 to accumulate in ER regions closely associated with the plasma membrane. The Journal of Cell Biology. 2006 Sept 11;174(6):803–13.

74. Palmer AE, Jin C, Reed JC, Tsien RY. Bcl-2-mediated alterations in endoplasmic reticulum Ca^{2+} analyzed with an improved genetically encoded fluorescent sensor. Proc Natl Acad Sci USA. 2004 Dec 14;101(50):17404–9.

75. Parekh AB, Putney JW. Store-Operated Calcium Channels. Physiological Reviews. 2005 Apr;85(2):757–810.

76. Ahuja M, Schwartz DM, Tandon M, Son A, Zeng M, Swaim W, et al. Orai1-Mediated Antimicrobial Secretion from Pancreatic Acini Shapes the Gut Microbiome and Regulates Gut Innate Immunity. Cell Metabolism. 2017 Mar;25(3):635–46.

77. Pallagi P, Madácsy T, Varga Á, Maléth J. Intracellular Ca2+ Signalling in the Pathogenesis of Acute Pancreatitis: Recent Advances and Translational Perspectives. IJMS. 2020 June 3;21(11):4005.

78. Sorin A, Rosas G, Rao R. PMR1, a Ca2+-ATPase in Yeast Golgi, Has Properties Distinct from Sarco/endoplasmic Reticulum and Plasma Membrane Calcium Pumps. Journal of Biological Chemistry. 1997 Apr;272(15):9895–901.

79. Vanoevelen J, Dode L, Van Baelen K, Fairclough RJ, Missiaen L, Raeymaekers L, et al. The Secretory Pathway Ca2+/Mn2+-ATPase 2 Is a Golgi-localized Pump with High Affinity for Ca2+ Ions. Journal of Biological Chemistry. 2005 June;280(24):22800–8.

80. Fenech MA, Sullivan CM, Ferreira LT, Mehmood R, MacDonald WA, Stathopulos PB, et al. *Atp2c2* Is Transcribed From a Unique Transcriptional Start Site in Mouse Pancreatic Acinar Cells. Journal Cellular Physiology. 2016 Dec;231(12):2768–78.

81. Fenech MA, Carter MM, Stathopulos PB, Pin CL. The pancreas-specific form of secretory pathway calcium ATPase 2 regulates multiple pathways involved in calcium homeostasis. Biochimica et Biophysica Acta (BBA) - Molecular Cell Research. 2020 Jan;1867(1):118567.

82. Uhlén M, Fagerberg L, Hallström BM, Lindskog C, Oksvold P, Mardinoglu A, et al. Tissue-based map of the human proteome. Science. 2015 Jan 23;347(6220):1260419.

83. Wu MM, Covington ED, Lewis RS. Single-molecule analysis of diffusion and trapping of STIM1 and Orai1 at endoplasmic reticulum–plasma membrane junctions. Lippincott-Schwartz J, Lippincott-Schwartz J, editors. MBoC. 2014 Nov 5;25(22):3672–85.

84. Chang CL, Hsieh TS, Yang TT, Rothberg KG, Azizoglu DB, Volk E, et al. Feedback Regulation of Receptor-Induced Ca2+ Signaling Mediated by E-Syt1 and Nir2 at Endoplasmic Reticulum-Plasma Membrane Junctions. Cell Reports. 2013 Nov;5(3):813–25.

85. Balghi H, Robert R, Rappaz B, Zhang X, Wohlhuter-Haddad A, Evagelidis A, et al. Enhanced Ca^{2+} entry due to Orai1 plasma membrane insertion increases IL-8 secretion by cystic fibrosis airways. FASEB j. 2011 Dec;25(12):4274–91.

86. Shan J, Liao J, Huang J, Robert R, Palmer ML, Fahrenkrug SC, et al. Bicarbonate-dependent chloride transport drives fluid secretion by the human airway epithelial cell line Calu-3. The Journal of Physiology. 2012 Nov;590(21):5273–97.

87. Balázs A, Rubil T, Wong CK, Berger J, Drescher M, Seidel K, et al. The potentiator ivacaftor is essential for pharmacological restoration of F508del-CFTR function and mucociliary clearance in cystic fibrosis. JCI Insight. 2025 May 22;10(10):e187951.

88. Pallagi P, Görög M, Papp N, Madácsy T, Varga Á, Crul T, et al. Bile acid- and ethanol-mediated activation of Orai1 damages pancreatic ductal secretion in acute pancreatitis. The Journal of Physiology. 2022 Apr;600(7):1631–50.

89. Wen L, Voronina S, Javed MA, Awais M, Szatmary P, Latawiec D, et al. Inhibitors of ORAI1 Prevent Cytosolic Calcium-Associated Injury of Human Pancreatic Acinar Cells and Acute Pancreatitis in 3 Mouse Models. Gastroenterology. 2015 Aug;149(2):481-492.e7.

90. Gidalevitz T, Prahlad V, Morimoto RI. The Stress of Protein Misfolding: From Single Cells to Multicellular Organisms. Cold Spring Harbor Perspectives in Biology. 2011 June 1;3(6):a009704–a009704.

91. Halls ML, Cooper DMF. Regulation by Ca2+-Signaling Pathways of Adenylyl Cyclases. Cold Spring Harbor Perspectives in Biology. 2011 Jan 1;3(1):a004143–a004143.

92. Park HW, Nam JH, Kim JY, Namkung W, Yoon JS, Lee J, et al. Dynamic Regulation of CFTR Bicarbonate Permeability by [Cl−]i and Its Role in Pancreatic Bicarbonate Secretion. Gastroenterology. 2010 Aug;139(2):620–31.

93. Sabbatini ME, D'Alecy L, Lentz SI, Tang T, Williams JA. Adenylyl cyclase 6 mediates the action of cyclic AMP-dependent secretagogues in mouse pancreatic exocrine cells via protein kinase A pathway activation. The Journal of Physiology. 2013 Aug;591(15):3693–707.

94. Willoughby D, Everett KL, Halls ML, Pacheco J, Skroblin P, Vaca L, et al. Direct Binding Between Orai1 and AC8 Mediates Dynamic Interplay Between Ca^{2+} and cAMP Signaling. Sci Signal [Internet]. 2012 Apr 10 [cited 2025 Nov 11];5(219). Available from: https://www.science.org/doi/10.1126/scisignal.2002299

95. Lefkimmiatis K, Srikanthan M, Maiellaro I, Moyer MP, Curci S, Hofer AM. Store-operated cyclic AMP signalling mediated by STIM1. Nat Cell Biol. 2009 Apr;11(4):433–42.

96. Lérias J, Pinto M, Benedetto R, Schreiber R, Amaral M, Aureli M, et al. Compartmentalized crosstalk of CFTR and TMEM16A (ANO1) through EPAC1 and ADCY1. Cellular Signalling. 2018 Apr;44:10–9.

97. Cooper DMF. Store-operated Ca2+-entry and adenylyl cyclase. Cell Calcium. 2015 Oct;58(4):368–75.

98. Johnstone TB, Agarwal SR, Harvey RD, Ostrom RS. cAMP Signaling Compartmentation: Adenylyl Cyclases as Anchors of Dynamic Signaling Complexes. Molecular Pharmacology. 2018 Apr;93(4):270–6.

99. Abu-Arish A, Pandzic E, Goepp J, Matthes E, Hanrahan JW, Wiseman PW. Cholesterol Modulates CFTR Confinement in the Plasma Membrane of Primary Epithelial Cells. Biophysical Journal. 2015 July;109(1):85–94.

100. Sarkar P, Lüscher BP, Ye Z, Chung WY, Abtahi AM, Zheng C, et al. Lipid transporters E-Syt3 and ORP5 regulate epithelial ion transport by controlling phosphatidylserine enrichment at ER/PM junctions. EMBO J. 2025 May 27;44(13):3697–719.

101. Cross BM, Breitwieser GE, Reinhardt TA, Rao R. Cellular calcium dynamics in lactation and breast cancer: from physiology to pathology. American Journal of Physiology-Cell Physiology. 2014 Mar 15;306(6):C515–26.

102. Strubberg AM, Liu J, Walker NM, Stefanski CD, MacLeod RJ, Magness ST, et al. Cftr Modulates Wnt/β-Catenin Signaling and Stem Cell Proliferation in Murine Intestine. Cellular and Molecular Gastroenterology and Hepatology. 2018;5(3):253–71.

103. Hammad AS, Machaca K. Store Operated Calcium Entry in Cell Migration and Cancer Metastasis. Cells. 2021 May 19;10(5):1246.